JOURNAL OF VIROLOGY, Aug. 2007, p. 8421–8438 Vol. 81, No. 16
0022-538X/07/$08.00+0 doi:10.1128/JVI.02641-06

Characterization of Rift Valley Fever Virus Transcriptional Terminations[▽]

Tetsuro Ikegami,[1] Sungyong Won,[1] C. J. Peters,[1,2] and Shinji Makino[1]*

Departments of Microbiology and Immunology[1] and Pathology,[2] University of Texas Medical Branch at Galveston, Galveston, Texas 77555-1019

Received 29 November 2006/Accepted 17 May 2007

Rift Valley fever virus (RVFV) (genus *Phlebovirus*, family *Bunyaviridae*) has a tripartite negative-strand genome and causes a mosquito-borne disease among humans and livestock in sub-Saharan African and Arabian Peninsula countries. Phlebovirus L, M, and N mRNAs are synthesized from the virus-sense RNA segments, while NSs mRNA is transcribed from the anti-virus-sense S segment. The present study determined the 3′ termini of all RVFV mRNAs. The 3′ termini of N and NSs mRNAs were mapped within the S-segment intergenic region and were complementary to each other by 30 to 60 nucleotides. The termini of M and L mRNAs were mapped within 122 to 107 nucleotides and 16 to 41 nucleotides, respectively, from the 5′ ends of their templates. Viral RNA elements that control phlebovirus transcriptional terminations are largely unknown. Our studies suggested the importance of a pentanucleotide sequence, CGUCG, for N, NSs, and M mRNA transcription terminations. Homopolymeric tracts of C sequences, which were located upstream of the pentanucleotide sequence, promoted N and M mRNA terminations. Likewise, the homopolymeric tracts of G sequences that are found upstream of the pentanucleotide sequence promoted NSs mRNA termination. The L-segment 5′-untranslated region (L-5′ UTR) had neither the pentanucleotide sequence nor homopolymeric sequences, yet replacement of the S-segment intergenic region with the L-5′ UTR exerted N mRNA termination in an infectious virus. The L-5′ UTR contained two 13-nucleotide-long complete complementary sequences, and their sequence complementarities were important for L mRNA termination. A computer-mediated RNA secondary structure analysis further suggested that RNA secondary structures formed by the sections of the two 13-nucleotide-long sequences and by the sequence between them may have a role in L mRNA termination. Our data demonstrated that viral RNA elements that govern L mRNA termination differed from those that regulate mRNA terminations in the M and S segments.

The family *Bunyaviridae* is composed of five genera: *Bunyavirus*, *Hantavirus*, *Nairovirus*, *Tospovirus*, and *Phlebovirus.* The latter includes Rift Valley fever virus (RVFV), Toscana virus (TOSV), sandfly fever Sicilian virus, Punta Toro virus (PTV), and Uukuniemi virus (UUKV). RVFV causes a disease endemic to sub-Saharan Africa that has emerged in explosive, mosquito-borne epidemics that have resulted in massive economic loss of sheep and cattle, while also causing hemorrhagic fever, encephalitis, retinal vasculitis, and lesser diseases in humans (40). Since the late 1970s, several large outbreaks of Rift Valley fever have occurred outside of sub-Saharan Africa, e.g., in Egypt (36), Madagascar (37), Saudi Arabia, and Yemen (2, 43).

RVFV has a tripartite negative-strand RNA genome, designated S, M, and L segments (42). In infected cells, the S segment uses an ambisense strategy to express the N and NSs proteins; N mRNA encoding N protein is transcribed from the virus-sense S segment, while NSs mRNA encoding NSs protein is transcribed from the anti-virus-sense S segment. The anti-virus sense of the M segment has a single open reading frame (ORF) and four proteins, namely, 78-kD, NSm, Gn, and Gc, that are translated from M mRNA (42). The anti-virus sense of the L segment also has a single ORF, which encodes L protein, a viral RNA-dependent RNA polymerase. N and L proteins are required for RVFV RNA synthesis (25, 35). Gn and Gc proteins are believed to be essential for binding to an as-yet-unidentified RVFV receptor, while both 78-kD and NSm proteins are dispensable for RVFV replication in cultured cells (19, 47). NSs protein inhibits host transcription by interacting with the p44 subunit of TFIIH, an essential transcriptional factor for cellular RNA polymerase II (34), and is a major viral virulence factor (8). However, it is not essential for RVFV replication in cell cultures (26, 38).

Faithful copies of virus-sense and anti-virus-sense RNAs are produced from their templates in bunyavirus-infected cells, whereas viral mRNAs are not faithful copies of the templates. Both virus-sense and anti-virus-sense RNAs lack a 5′-end cap structure, while viral mRNAs carry a cap structure at their 5′ end; like orthomyxoviruses and arenaviruses, bunyavirus RNA polymerase cleaves off the 5′ cap structure of host mRNAs and uses it as a primer for viral mRNA synthesis (17, 23, 30, 31, 41, 44). Past studies showed that bunyavirus mRNAs lack the 3′-end poly(A) tract (9, 10, 12, 39), with the exception of the mRNA from the M segment of Sin Nombre virus, a hantavirus (24). The N and NSs mRNAs of phleboviruses are substantially shorter than the mRNAs of their templates, because transcription of both mRNAs is terminated within the intergenic region (S-IGR), which is located between the N and NSs ORFs (42). The 3′ ends of the N and NSs mRNAs have been identified in several phleboviruses (12, 21, 44). The transcriptional termination sites of the M mRNA of snowshoe hare virus (13), Germiston virus (9), Sin Nombre virus (24), and RVFV (11) are shorter by about 60, 80, 70, and 112 nucleotides (nt), respectively, than that of the anti-virus-sense M segment, sug-

* Corresponding author. Mailing address: Department of Microbiology and Immunology, University of Texas Medical Branch, Galveston, TX 77555-1019. Phone: (409) 772-2323. Fax: (409) 772-5065. E-mail: shmakino@utmb.edu.

▽ Published ahead of print on 30 May 2007.

gesting that viral M mRNA synthesis terminates within the 5′-end untranslated region (5′ UTR) of the template RNA. Recently, Albarino et al. reported the exact termini of N, NSs, and M mRNAs of three phleboviruses, including RVFV, Toscana virus, and sandfly fever Sicilian virus, by 3′ rapid amplification of cDNA ends (3′RACE) analysis, and they found that all mRNA termini exist immediately upstream of the conserved sequence 3′-C_{1-3}GUCG/A-5′ (1). Their data further suggested that the 3′ end of the RVFV L mRNA is identical to that of the anti-virus-sense genomic L-segment RNA and speculated that the L mRNA is synthesized by runoff of viral polymerase (1). Another study reported that the 3′ end of the L mRNA of Sin Nombre virus, a hantavirus, is also the full-length complement of the 5′ end of the viral L RNA segment (24). Viral RNA signals that play critical roles in transcription terminations are largely unknown in any of the phleboviruses.

The present study determined the 3′ termini of all RVFV mRNAs by using an RNase protection assay (RPA) and characterized the viral RNA elements involved in the viral mRNA transcription terminations.

MATERIALS AND METHODS

Cells and viruses. Vero E6 cells were maintained in Dulbecco's modified minimum essential medium (Invitrogen, Carlsbad, CA) containing 10% fetal bovine serum. BHK/T7-9 cells, which stably express T7 RNA polymerase (28), were grown in minimal essential medium alpha (Invitrogen) containing 10% fetal bovine serum. Penicillin (100 U/ml) and streptomycin (100 μg/ml) (Invitrogen) were added to the media. BHK/T7-9 cells were selected in medium containing 600 μg/ml hygromycin (Cellgro). An RVFV vaccine candidate, MP-12, was used for all of the experiments, and infectivity was assayed by plaque assay with Vero E6 cells.

Plasmid constructions. Standard molecular biology techniques, including a PCR-based mutagenesis method, were used for plasmid constructions. A plasmid was constructed by introducing the XhoI site between the N gene ORF and S-IGR and the SpeI site between the *Renilla* luciferase (rLuc) ORF and S-IGR of pPro-T7-S(+)rLuc (26). pPro-T7-S(+)rLuc-LUTR then was constructed by replacing the S-IGR of this newly constructed plasmid with a PCR fragment of the 5′ UTR of the L segment (L-5′ UTR), which corresponded to nt 6298 to 6396 from the 3′ end of the virus sense. The pPro-T7-mSv plasmid was constructed to contain the following elements in the 5′ to 3′ direction: T7 promoter; the 5′ UTR of the virus sense S segment (S-5′ UTR); the first 172-nt region of the NSs gene ORF, with the first ATG being replaced by TAG; a multicloning site containing SpeI, XhoI, and BamHI; the full-length antisense rLuc ORF; the 3′ UTR of the virus-sense S segment; and the hepatitis delta virus (HDV) ribozyme sequence. The plasmids IGR-1, MUTR-1, and LUTR-1 were constructed by inserting the entire S-IGR plus a short sequence of the N gene ORF (nt 758 to 776 from the 3′ end of the virus-sense S segment) between the SpeI and BamHI sites of pPro-T7-mSv; the 5′ UTR of the virus-sense M segment (nt 3615 to 3877 from the 3′ end of the viral-sense M segment) between the SpeI and XhoI sites of pPro-T7-mSv; and the 5′ UTR of the virus-sense L segment (nt 6298 to 6396 from the 3′end of the viral-sense L segment) between the SpeI and XhoI sites of pPro-T7-mSv, respectively. IGR-1, MUTR-1, and LUTR-1 served as the parental plasmids for other mutants. Four different pSPT18 (Roche Applied Science)-derived plasmids were constructed for the preparation of in vitro-synthesized RNA probes. The N probe hybridized at nt 609 to 990 of the anti-virus-sense S segment; the NSs probe hybridized at nt 665 to 1036 of the virus-sense S segment; the M probe hybridized at nt 3545 to 3885 of the anti-virus-sense M segment; and the L probe hybridized at nt 6135 to 6404 of the anti-virus-sense L segment. Another pSPT18-derived plasmid encoding the LUTR probe, which specifically hybridized at nt 645 to 956 of the anti-virus-sense S segment of pPro-T7-S(+)rLuc-LUTR, was also produced. All of the constructs were confirmed to have the expected sequences.

Virus rescue. The MP-12 strain carrying L-5′ UTR in place of the S-IGR in the S segment (rMP12-LUTR) was recovered as described previously (26). Briefly, subconfluent monolayers of BHK/T7-9 cells were cotransfected with pPro-T7-S(+)rLuc-LUTR, pPro-T7-M(+), pPro-T7-L(+), pT7-IRES-vN, pCAGGS-vG, and pT7-IRES-vL using TransIT-LT1 (Mirus, Madison, WI). The culture medium was replaced with fresh medium 24 h later. At 5 days posttransfection, the culture supernatants were collected, clarified, and then inoculated into Vero E6 cells. The supernatant of infected Vero E6 cells at 3 days postinfection (p.i.) was used for the experiment.

RPA. The N probe, NSs probe, M probe, L probe, and LUTR probe were synthesized in vitro from four different plasmids by using T7 RNA polymerase (multiprobe RPA system; BD Biosciences) in the presence of [α-^{32}P]UTP. Vero E6 cells were infected with the MP-12 strain at a multiplicity of infection of 1.0. Total RNA was extracted at 6 h p.i. and mixed with ^{32}P-labeled N, NSs, M, or L probe. Total RNA from rMP12-LUTR-infected Vero E6 cells was mixed with the LUTR probe. The full-length, anti-virus-sense S RNA transcripts, the virus-sense S RNA transcripts, the anti-virus-sense M RNA transcripts, and the anti-virus-sense L RNA transcripts were synthesized in vitro from linearized pProT7-S(+), pProT7-S(−), pProT7-M(+), and pProT7-L(+) (26, 27), respectively, and used as control RNAs. The RPA was performed as described previously (27), and the protected RNAs were analyzed on a 4.75% polyacrylamide gel containing 8 M urea. Undigested probes and multiprobe template hCK-3 (RiboQuant RPA kit; BD Biosciences) served as size markers.

Minigenome system. Subconfluent monolayers of BHK/T7-9 cells in 6-well plates were cotransfected with 1.5 μg of one of the pPro-T7-mSv-derived minigenome plasmids, 1 μg of pT7-IRES-vN, 1 μg of pCAGGS-vG, and 0.5 μg of pT7-IRES-vL using TransIT-LT1. At 48 h posttransfection, total RNAs were extracted using TRIzol reagent (Invitrogen).

Northern (RNA) blotting. Two micrograms of total RNA was denatured and separated on 1.5% denaturing agarose-formaldehyde gels and transferred onto a nylon membrane (Roche Applied Science). Northern blot analysis was performed as described previously (25) with strand-specific RNA probes (27).

Computer-based RNA folding analysis. The RNA folding prediction was performed using Mfold3.2 (48).

RESULTS

Identification of the 3′ termini of MP-12 mRNAs. We employed RPA to determine the 3′ termini of all of the mRNAs of the MP-12 strain of RVFV. Double-stranded RNAs were generated after RNase digestion of the mixture of total intracellular RNAs from MP-12-infected cells and each of the radiolabeled N, NSs, M, and L probes and then were separated on a denatured polyacrylamide gel. We expected that each probe would hybridize with one of the full-length viral RNAs as well as with one of the viral mRNAs (Fig. 1). For example, if the 3′ end of M mRNA is truncated compared to that of the anti-virus-sense M segment, then RPA would generate two signals of different sizes; a large signal would be produced from the hybrid of the probe, and the anti-virus-sense M segment and a small signal would be made from the hybrid of the probe and M mRNA. The differences in the sizes of these two signals would indicate the 3′ termini of M mRNA. The same expectation was applied to N, NSs, and L mRNA. Because the 3′ termini of N and NSs mRNAs of other phleboviruses are mapped within the S-IGR (12, 21, 44), we expected that the RPA using the N probe would generate two signals and that their size differences would indicate the 3′ ends of N mRNAs. This expectation also applied to NSs mRNA.

Total intracellular RNAs extracted from MP-12-infected Vero E6 cells at 6 h p.i. were mixed with each probe, and RPA was performed (Fig. 2). RNase-treated samples of the hybrid of in vitro-transcribed, full-length anti-virus-sense S RNA transcripts (Fig. 2A, lane iSvc) and N probe (Fig. 2A, lane P), as well as hybrids of the virus-sense S RNA transcripts (Fig. 2B, lane iSv) and NSs probe (Fig. 2B, lane P), the anti-virus-sense M RNA transcripts (Fig. 2C, lane iMvc) and M probe (Fig. 2C, lane P), and the anti-virus-sense L RNA transcripts (Fig. 2D, lane iLvc) and L probe (Fig. 2D, lane P), were included in the

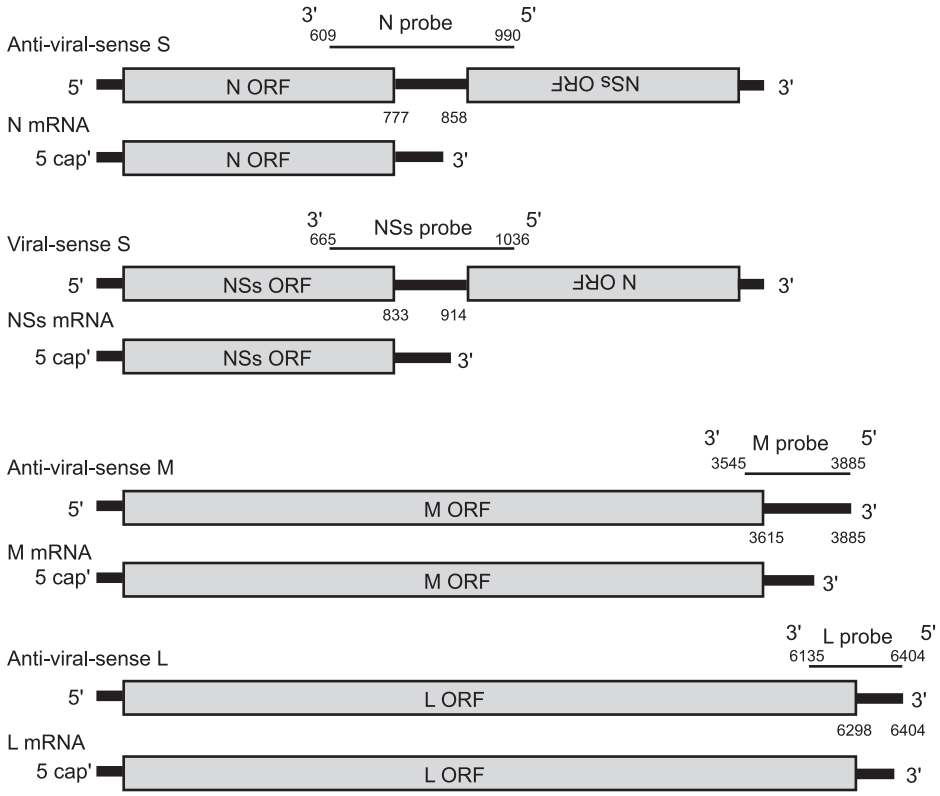

FIG. 1. Schematic representation of strand-specific RNA probes that were used for the detection of RVFV mRNAs by an RPA. Shown are the binding sites of each probe to virus-sense or anti-virus-sense RNAs and the nucleotide positions of the intergenic region on anti-virus-sense S and virus-sense S segments, the UTR of anti-virus-sense M segment, and the UTR of anti-virus-sense L segment.

RPA as controls. Multiprobe hCK-3 served as a size marker (Fig. 2, lanes hCK-3). As expected, no RNase-resistant signals were detected in the samples using total RNAs from mock-infected cells and yeast tRNA (Fig. 2, lanes M and Y). In a given probe, RPA using in vitro-synthesized RNA transcripts and RPA using RNAs from infected cells produced a slowly migrating signal of the same size, which represented an anti-virus-sense S segment (Fig. 2A, Svc), a virus-sense S segment (Fig. 2B, Sv), an anti-virus-sense M segment (Fig. 2C, Mvc), or an anti-virus-sense L segment (Fig. 2D, Lvc). Clear identification of the anti-virus-sense S-segment signal required the use of a larger amount of intracellular RNAs (Fig. 2A, lane I*). In addition, for a given probe, the RPA using intracellular RNAs from infected cells, but not in vitro-synthesized RNA transcripts, generated a fast-migrating major signal that corresponded to viral mRNA (Fig. 2, lanes I). The signals of N mRNA appeared as two closely migrating bands differing in length by approximately 5 nt (Fig. 2A, lane I), suggesting that the N mRNA was a mixture of two major mRNA subspecies, one of which lacked ~5 nt of the 3′-end sequence of the other N mRNA subspecies. Also, the NSs mRNA appeared to have a major mRNA subspecies and a minor mRNA subspecies, the latter of which had ~5 nt shorter 3′ termini than the former. Often, the L mRNA-derived signal appeared as a minor signal. Several minor signals also were detected in the RPA using intracellular RNAs; they may be produced by hybridizing small amounts of truncated probes with viral mRNAs or may represent degraded viral RNAs and/or minor viral mRNA species. To estimate the sizes of the mRNAs, standard curves were plotted on semilog graphs based on the migration of the multiprobe (hCK-3) as a size marker. The termini of N, NSs, M, and L mRNAs then were calculated on the basis of the standard curves (Fig. 2, right panels); the *x* axes show migrations (in centimeters) of the signals of the undigested probes, those of the viral genomic RNAs, and those of the viral mRNAs from the top of the gels. We performed at least three independent experiments for each probe, and the termini of viral mRNAs were determined within a window of 16 to 26 nucleotides (Fig. 3A to C); the 3′ termini of the N and NSs mRNAs were complementary to each other by 30 to 60 nt, while the 3′ end of the M mRNA was mapped from 122 to 107 nt upstream of the 5′ end of the template RNA; the L mRNA 3′ terminus appeared to be only 21 to 41 nt from the 5′ end of its template.

Past studies on other bunyaviruses, including those with PTV (12), Germiston virus (9, 10), and Akabane virus (39), reported that the 3′ termini of bunyavirus mRNAs lacked a poly(A) tract. Thus far, the glycoprotein precursor mRNA (which is the equivalent of the M mRNA of phleboviruses) of Sin Nombre virus, a hantavirus, is the only bunyavirus mRNA found to have a nontemplated poly(A) sequence at the 3′ end (24). To know whether MP-12 mRNAs carry poly(A) tracts at their 3′ termini, we tested binding of MP-12 mRNAs to an oligo(dT) cellulose and found that they did not bind efficiently to an oligo(dT) column, whereas murine coronavirus mRNAs carrying the 3′-end poly(A) tract (33) efficiently bound to an oligo(dT) column (data not shown). Furthermore, we failed to

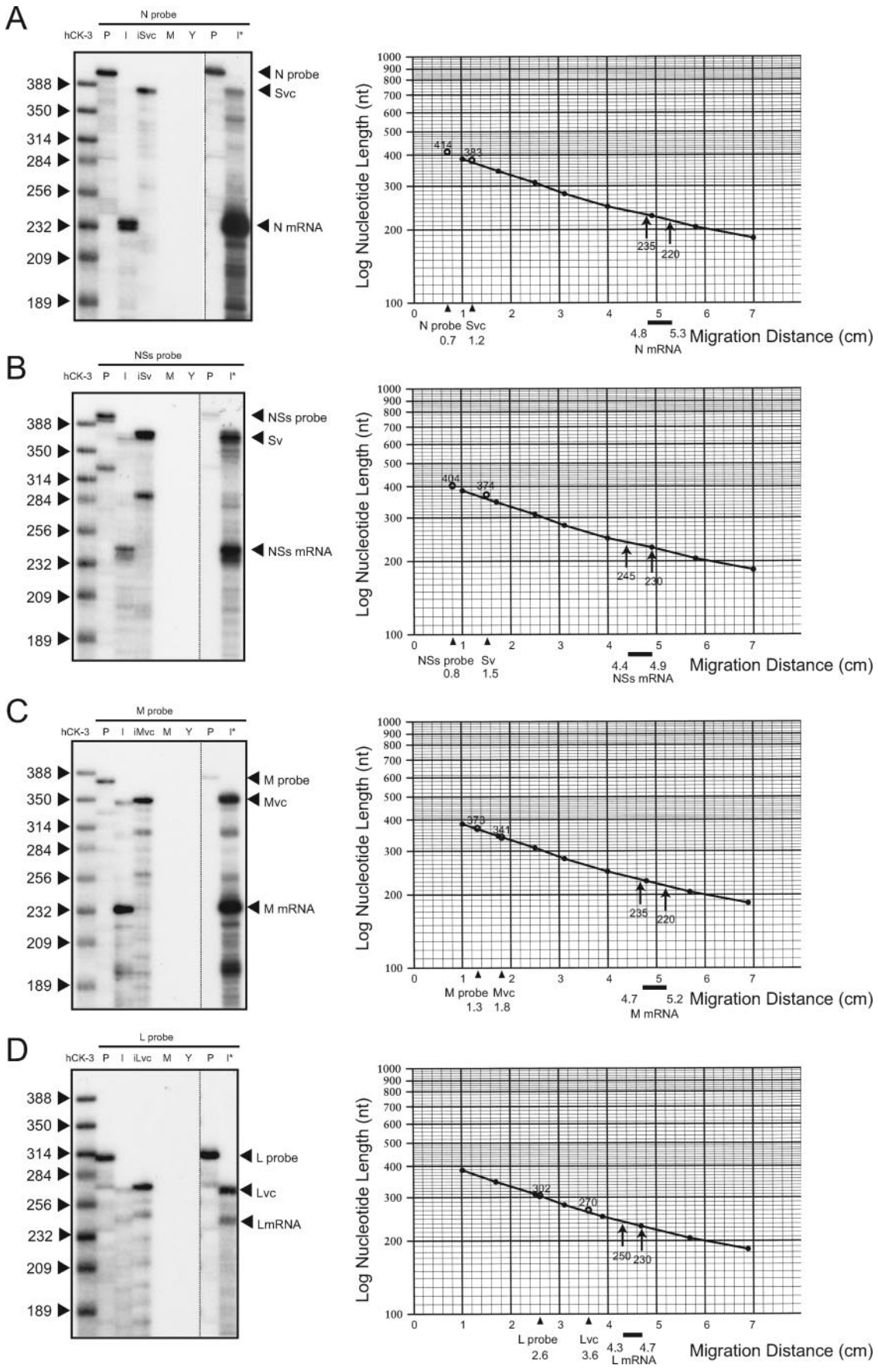

FIG. 2. RPA of the 3′ termini of N, NSs, M, and L mRNAs. Total intracellular RNA from mock-infected Vero E6 cells (M) and that from MP-12-infected Vero E6 cells (I); yeast tRNA (Y); in vitro-transcribed, anti-virus-sense S RNA (iSvc); in vitro-transcribed, virus-sense S RNA

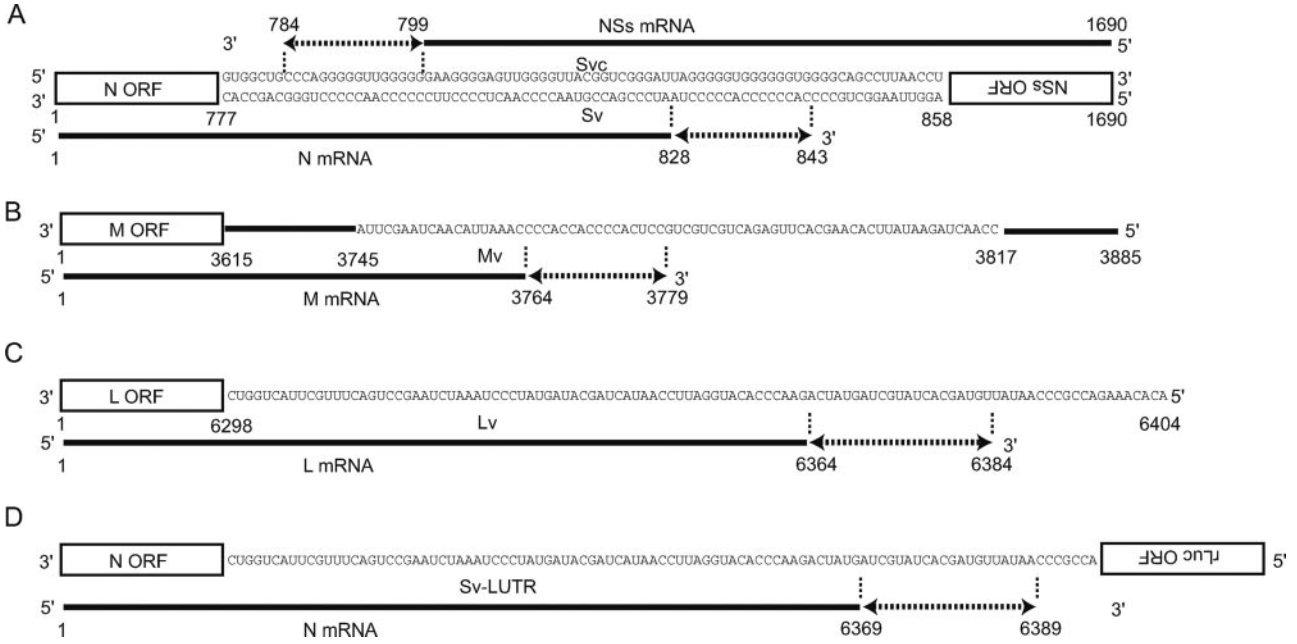

FIG. 3. Mapping of the viral mRNA termini. The termini of N and NSs mRNAs (A), M mRNA (B), and L mRNA (C) are shown with their locations relative to the virus-sense S segment (Sv); the anti-virus-sense S segment (Svc); the virus-sense M segment (Mv); and the virus-sense L segment (Lv), respectively. The termini of each mRNA reside within the dotted lines with terminal arrows. (D) The terminus of the viral N mRNA of rMP12-LUTR, which contained a 5′ UTR in place of the S-IGR (see the text and the legend to Fig. 4). Also shown are the nucleotide positions of the N-5′ UTR, the M-5′ UTR, and the L-5′ UTR from the 3′ ends of the virus-sense S segment, M segment, and L segment, respectively, and those of the NSs-5′ UTR from the 3′ end of the anti-virus-sense S segment.

obtain PCR products by 3′RACE using an oligo(dT) primer and primers that bound near the 3′ termini of viral mRNA sequences, and yet the PCR products were obtained after polyadenylation of viral mRNAs by yeast poly(A) polymerase. These data strongly suggested that the RVFV mRNAs were not polyadenylated at the 3′ termini.

Further characterization of the 3′ terminus of L mRNA. To further establish the L mRNA 3′ end, we generated an MP-12-derived virus, rMP12-LUTR, which contained most of the L-5′ UTR region (nt 6298 to 6396) and rLuc ORF in place of the S-IGR and the NSs ORF, respectively, in the S segment (Fig. 4A). The very 5′-end 8 nt were missing from the inserted L-5′ UTR region to prevent a possible accumulation of a novel replicating RNA segment consisting of the S-3′ UTR, the N ORF, and the complete L-5′ UTR. If the L-5′ UTR carries an L mRNA transcription termination signal(s) that exerts its function in the S segment, then the replacement of the S-IGR with the L-5′ UTR in rMP12-LUTR would result in transcriptional termination of the N mRNA. Identifying the 3′ end of the N mRNA of rMP12-LUTR would further confirm the MP-12 L mRNA terminus.

After successful recovery of rMP12-LUTR by using a reverse genetics system (26), intracellular RNAs were extracted from mock-infected Vero E6 cells or Vero E6 cells that were independently infected with MP-12, rMP12-LUTR, or rMP12-rLuc, the latter of which carries the rLuc ORF in the place of the NSs ORF (26). Northern blot analysis of intracellular RNAs using an N antisense probe that hybridized with the N mRNA and anti-virus-sense S segment and an rLuc antisense probe that hybridized with the rLuc mRNA and the virus-sense S segment showed efficient replication of the S-segment RNA in all of the infected samples (Fig. 4B). Synthesis of N and rLuc mRNAs occurred in rMP12-rLuc-infected cells. N mRNA synthesis also occurred in rMP12-LUTR-infected cells, demonstrating that replacement of the S-IGR with the L-5′ UTR resulted in N mRNA transcriptional termination. Efficient rLuc mRNA accumulation occurred in rMP12-rLuc-infected cells, whereas the abundance of rLuc mRNAs was substantially less in rMP12-LUTR-infected cells, suggesting that the L-5′ UTR exerted efficient transcriptional termination only in the virus-sense orientation.

The RPA using intracellular RNAs from rMP12-LUTR-infected cells and the LUTR probe, which hybridizes with the 3′ region of the N mRNA and anti-virus-sense S RNA of

(iSv); in vitro-transcribed, anti-virus-sense M RNA (iMvc); or in vitro-transcribed, anti-virus-sense L RNA (iLvc) were mixed with radiolabeled N probe (A), NSs probe (B), M probe (C), or L probe (D), and RPAs were performed (left panels). A commercially available multiprobe (hCK-3) served as a size marker. An undigested probe that was used for each RPA was also applied to the gel (P). Lanes I* used larger amounts of RNA from infected cells. Standard curves were plotted on semilog graphs based on the migration of the hCK-3 marker (right panels). The *x* axes show migrations (in centimeters) of the signals of the undigested probes, those of the viral genomic RNAs, and those of the viral mRNAs from the top of the gels.

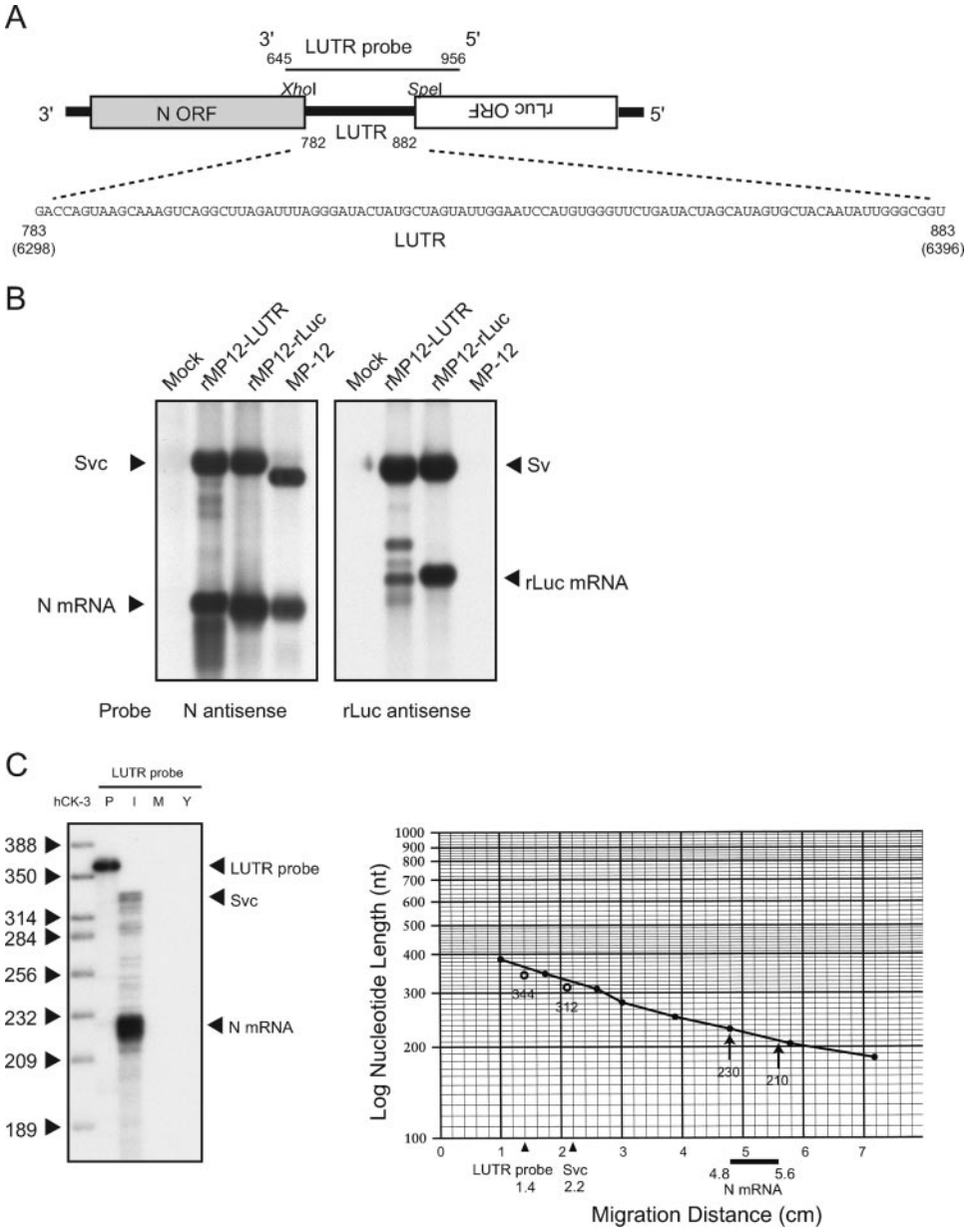

FIG. 4. Analysis of the L mRNA termination site using rMP12-LUTR. (A) Schematic diagram of the S segment of rMP12-LUTR, which contained the L-5′ UTR (nt 6298 to 6396 from the 3′ end of the virus sense) in place of the S-IGR and the rLuc ORF in place of the NSs gene ORF. A strand-specific RNA probe (LUTR probe) was designed to bind to the virus-sense S RNA of rMP12-LUTR at nt 645 to 956 from the 3′ end of the virus-sense S segment. (B) Northern blot analysis was performed to detect anti-virus-sense S RNA, N mRNA, and rLuc mRNA using intracellular RNAs from mock-infected Vero E6 cells, rMP12-LUTR-infected Vero E6 cells, rMP12-rLuc-infected Vero E6 cells, and MP-12-infected Vero E6 cells. The N antisense probe bound to the N gene ORF, while the rLuc antisense probe bound to the rLuc gene ORF. Sv, virus-sense S segment; Svc, anti-virus-sense S segment. (C) RPA was performed to identify the termination site of the N mRNA transcribed in rMP12-LUTR-infected cells (left panel). For RPA, we used intracellular RNAs from mock-infected Vero E6 cells (M) and rMP12-LUTR-infected Vero E6 cells (I) as well as yeast tRNA (Y) with a radiolabeled LUTR probe. An undigested radiolabeled probe was also applied to the gel (P), and hCK-3 served as a size marker. The right panel shows a standard curve made by the hCK-3 marker. The migration distances (in centimeters) of the undigested probe, the protected viral S-segment signal, and the protected mRNA signal from the top of the gel are shown on the *x* axis.

rMP12-LUTR (Fig. 4A), identified the 3′ end of the N mRNA at nt 6369 to 6389 of the L-5′ UTR (Fig. 4C). The L mRNA 3′ terminus, which was determined with experiments depicted in Fig. 2D, and the rMP12-LUTR N mRNA 3′ terminus were mapped within the 20-nt window, and they overlapped by 15 nt (Fig. 3C and D), strongly suggesting that the 3′ end of the MP-12 L mRNA, which was determined by RPA using an L probe, was correct. These experiments further suggested that an RNA element(s) that controls L mRNA transcriptional termination resided within the L-5′ UTR, and sequences outside of the L-5′ UTR had little, if any, effect on L mRNA transcription termination.

A

RVFV N-5'UTR	821	AGCCCUAAUC CCCCACCCCC CACCCCGUCG GAAUU	853
RVFV NSs-5'UTR	809	UGAGGGGAAG GGGGGUUGGG GGACCCGUCG GUGAA	775
RVFV M-5'UTR	3757	AUUAAACCCC ACCA- CCCCA CU- - CCGUCG UCGUC	3785

B

RVFV N-5'UTR	821	AGCCCUAAUC CCCCACCCCC CACCCCGUCG GAAUU	853
RVFV NSs-5'UTR	809	UGAGGGGAAG GGGGGUUGGG GGACCCGUCG GUGAA	775
TOSV N-5'UTR	867	UUCCCACCCA UCACCCCCCC UGAUCCGUCG GUGAA	901
TOSV NSs-5'UTR	1040	GUUAGGAUUA AGGGGAUUGG GGGACCGUCG AGUGA	1074
UUKV NSs-5'UTR	922	AGUCUAGUUA CUAGACUCCU GUCAACGUCG GACGA	956
PTV N-5'UTR	965	UUGUAACUGG GUGUCAGGGU GGACCCGUCG AAUAG	999

FIG. 5. Sequences of the template RNAs corresponding to the 3′ termini of viral mRNAs and their flanking regions. Shown is the alignment of the RVFV N-5′ UTR, RVFV NSs-5′ UTR, and RVFV M-5′ UTR (A) and that of the RVFV N-5′ UTR, RVFV NSs-5′ UTR, TOSV N-5′ UTR, TOSV NSs-5′ UTR, UUKV NSs-5′ UTR, and PTV N-5′ UTR (B). The transcriptional termination sites identified in this study or reported by others (12, 21, 44) are denoted by the shaded boxes. Numbers indicate the nucleotide positions of the N-5′ UTR and NSs-5′ UTR from the 3′ end of the virus-sense S segment and the M-5′ UTR from the 3′ end of the virus-sense M segment. The asterisks represent the conserved sequences among the RVFV RNAs listed in panel A and those among the viral RNAs listed in panel B.

Sequences of the template RNAs corresponding to the 3′ termini of viral mRNAs and their flanking regions. As a first step in identifying viral RNA elements that control viral mRNA termination, we compared sequences at the transcription termination sites and their flanking regions of the template RNAs and found the presence of homopolymeric C tracts in the template RNAs that corresponded to the 3′ termini of N and M mRNAs and homopolymeric G tracts in the anti-virus sense of the S segment that corresponded to the 3′ termini of the NSs mRNA (Fig. 5A). We also noted the presence of an 8-nt sequence, CCCGUCGG, at a region of the virus-sense S-IGR corresponding to the 3′ end of N mRNA (N-5′ UTR) and at that of the anti-virus-sense S-IGR corresponding to the 3′ end of the NSs mRNA (NSs-5′ UTR). A 6-nt sequence, CCGUCG, which is a part of the 8-nt sequence, was also detected in the template RNA that corresponded to the 3′-terminal region of the M mRNA (M-5′ UTR). Furthermore, the M-5′ UTR region had two partially overlapping pentanucleotides, CGUCG, which were a part of the 6-nt sequence within the sequence of CCGUCGUCG. Thus, the pentanucleotide sequence CGUCG was detected in the templates of the RNA corresponding to the termini of the N, NSs, and M mRNAs. Of note, the TOSV N-5′ UTR, TOSV NSs-5′ UTR, UUKV NSs-5′ UTR, and PTV N-5′ UTR also contained CGUCG pentanucleotides (Fig. 5B) (20), implying that the pentanucleotide sequence may have a role in the transcription termination of the N, NSs, and M mRNAs of the phleboviruses. In contrast, the RVFV L-5′ UTR had neither the pentanucleotide sequence nor the homopolymeric C or G tract (data not shown).

Development of a minigenome system for studying viral mRNA transcription terminations. To study viral transcription termination mechanisms, we established an RVFV minigenome system, in which minigenome mRNA transcription occurred from replicating minigenome RNA carrying the S-IGR, the M-5′ UTR, or the L-5′ UTR, and we tested the effects of altering the sequences within the S-IGR, the M-5′ UTR, or the L-5 ′UTR on minigenome mRNA transcription termination. To this end, we constructed the parental plasmid pPro-T7-mSv, expressing a virus-sense S-segment-like minigenome, which consisted of the 5′ UTR of the virus-sense S segment; the first 172-nt region of the NSs gene ORF, in which the first ATG was replaced by TAG; a multicloning site; the full-length antisense rLuc ORF; and the 3′ UTR of the virus-sense S segment (Fig. 6A, top). Several different series of pPro-T7-mSv-derived minigenomes, each of which contained an intact or mutated S-IGR, M-5′ UTR, or L-5′UTR at the multiple cloning site, were used to define the RNA elements that control the viral mRNA transcription termination in the cells coexpressing the N and L proteins.

The rationale for the use of pPro-T7-mSv-derived minigenomes for analysis of viral mRNA transcription termination was as follows. (i) Analysis of rMP12-LUTR showed that the L-5′ UTR exerted transcription termination in the S-segment-derived RNA. (ii) Preliminary studies showed that efficient accumulation of minigenome RNA, the size of which was comparable to that of pPro-T7-mSv-derived minigenomes, and its mRNA occurred in the presence of the N and L proteins, suggesting easy detection of the minigenome and its mRNA (data not shown). (iii) The rLuc-specific probe unambiguously identified rLuc mRNA from replicating pPro-T7-mSv-derived minigenomes and did not hybridize with mRNA transcripts encoding the N protein from the cotransfected N-protein expression plasmid. (iv) Replacement of the first AUG of a partial-length NSs ORF with a termination codon of UAG prevented accumulation of a truncated NSs protein, which might affect minigenome RNA synthesis (25). (v) Replacing the N ORF with the rLuc ORF prevented the synthesis of minigenome mRNA encoding the N protein, whose abundance may affect minigenome RNA synthesis and transcription (25). (vi) Finally, analysis of the M and L mRNA transcription termination mechanisms using an M-like minigenome and L-like minigenome, respectively, by introducing mutations at their 5′ UTRs may not be possible, because the introduced mutation may inhibit the minigenome replication (3, 5, 14–16, 18, 32).

Analysis of N mRNA transcription termination control. To identify RNA elements that control N mRNA termination, a plasmid, IGR-1, was constructed by inserting a sequence including the entire S-IGR and a short sequence of the N ORF (nt 758 to 858 from the 3′ end of the virus-sense S segment) at the multiple-cloning site of pPro-T7-mSv (Fig. 6A, bottom). BHK/T7-9 cells, stably expressing T7 RNA polymerase (28), were cotransfected with IGR-1, pT7-IRES-vN expressing N protein, and pT7-IRES-vL expressing L protein (25). The constitutively expressed T7 polymerase drove the expression of the RNA transcripts encoding the L and N proteins, leading to a cap-independent translation of N and L proteins, both of which in turn supported replication and transcription of the expressed IGR-1 minigenome. Total intracellular RNAs were collected at 48 h posttransfection. Northern blot analysis using a virus-sense rLuc probe demonstrated primary transcripts of the IGR-1 minigenome, which probably did not undergo RNA cleavage at the HDV ribozyme site, and the full-length, virus-sense IGR-1 minigenome of the expected size (Fig. 6B, bottom panel). Experiments using the anti-virus-sense rLuc probe revealed that coexpression of the N and L proteins resulted in IGR-1 RNA replication, while addition of pCAGGS-vG that expresses viral proteins encoded by the M ORF (26) had little

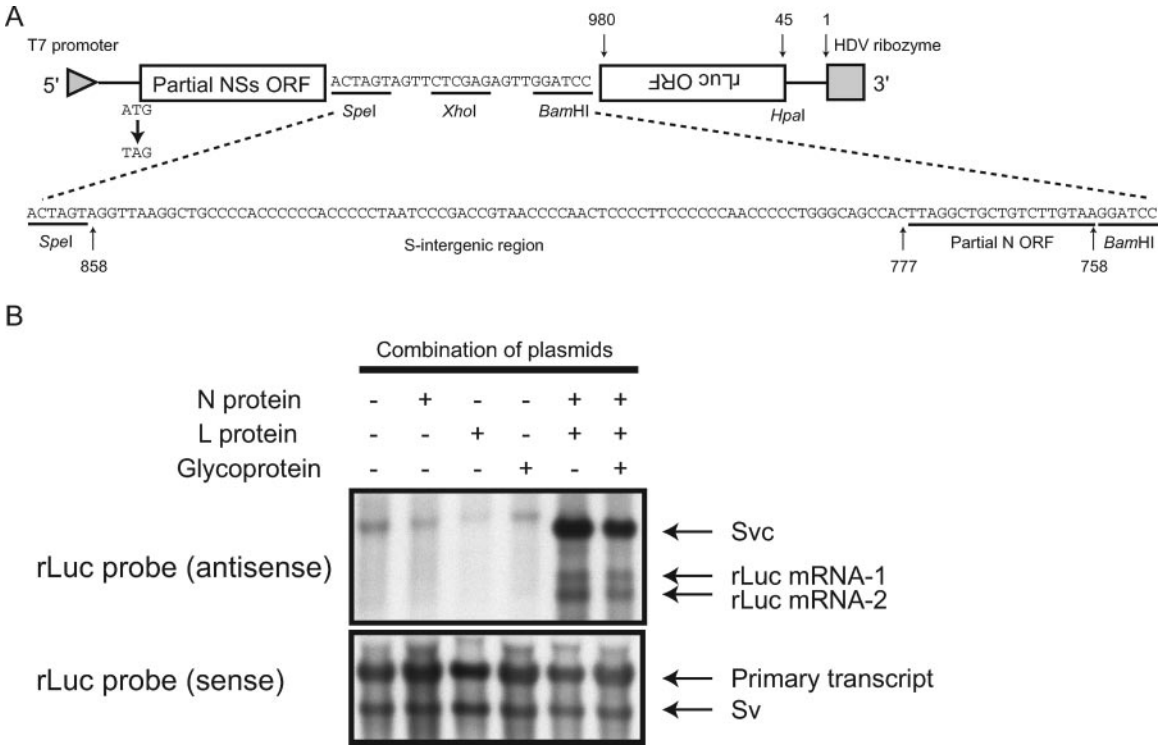

FIG. 6. Analysis of transcriptional termination using a minigenome system. (A) Schematic diagram of pPro-T7-mSv expressing an S-segment-like minigenome (top). The sequence shown at the bottom represents the inserted S-IGR in IGR-1. The nucleotide positions of the pPro-T7-mSv from the 3′ end of the virus-sense S-like minigenome and those of the S-intergenic region and the partial N ORF from the 3′ end of the virus-sense S segment are shown at the top and bottom, respectively. (B) Subconfluent BHK/T7-9 cells in 6-well plates were transfected with 1.5 μg of IGR-1, 1.0 μg of pT7-IRES-vN (N protein), 0.5 μg of pT7-IRES-vL (L protein), or 1.0 μg of pCAGGS-vG (Glycoprotein). At 48 h posttransfection, intracellular RNAs were extracted and analyzed by Northern blotting using strand-specific probes that bound to the sense rLuc gene ORF (antisense) or the antisense rLuc gene ORF (sense). The transcript without the self cleavage is shown along with the HDV ribozyme (primary transcript), the anti-virus-sense IGR-1 (Svc), the virus-sense IGR-1 (Sv), and two rLuc mRNAs (rLuc mRNA-1 and rLuc mRNA-2).

effect on IGR-1 accumulation. Furthermore, this probe detected two different lengths of rLuc mRNAs, which we denoted rLuc mRNA-1 and rLuc mRNA-2, suggesting the presence of two transcription termination sites within the virus-sense IGR-1 RNA.

As described above, the S-IGR carried the 8-nt complementary sequences CCCGUCGG and CCGACGGG (see the two boxed sequences in Fig. 7A) and homopolymeric C-tract sequences between them. To determine the importance of these RNA elements for transcription termination in the S-IGR, two series of IGR-1-derived deletion mutants were generated. The 8-nt sequence at nt 844 to 851 (Fig. 7A, right boxes) was deleted in IGR-2, IGR-3, IGR-4, IGR-5, and IGR-6. IGR-6 also lacked the 8-nt sequence CCGACGGG (Fig. 7A, left boxes) at nt 779 to 786. The second series of mutants, IGR-7 and IGR-8, had a deletion between the two complementary 8-nt sequences, including a region that corresponded to the 3′ terminus of N mRNA (Fig. 7A, dotted lines with terminal arrows). Synthesis of rLuc mRNA-1 and rLuc mRNA-2 occurred in the cells that underwent replication of IGR-1, IGR-7, and IGR-8; the size of rLuc mRNA-2 was the same among them, while the size of IGR-8 rLuc mRNA-1 was the smallest and that of IGR-1 rLuc mRNA-1 was the largest (Fig. 7A, right panel). Synthesis of rLuc mRNA-2 of the same size was detected in the cells supporting replication of IGR-2, IGR-3, IGR-4, and IGR-5 (Fig. 7A, left panel). Cells supporting IGR-6 replication accumulated neither rLuc mRNA-1 nor rLuc mRNA-2; a minor diffuse signal that migrated close to rLuc mRNA-2 in IGR-6 replicating cells (Fig. 7A, left panel) was not consistently detected. These data suggested that the 8-nt sequence at nt 844 to 851 and its complementary sequence at nt 779 to 796 were necessary for rLuc mRNA-1 termination and rLuc mRNA-2 termination, respectively. The data for IGR-5, IGR-7, and IGR-8 also suggested that most of the sequences, including the homopolymeric C tract, between the 8-nt sequences were dispensable for rLuc mRNA-2 termination.

The accumulation of rLuc mRNA-2, but not rLuc mRNA-1, after removal of the 8-nt sequence at nt 844 to 851 and the region corresponding to the 3′ terminus of the N mRNA led to speculation that the mechanism of rLuc mRNA-1 termination mimics the mechanism that exerted N mRNA transcription termination. To further establish the importance of two complementary 8-nt sequences for the rLuc mRNA-1 termination, we examined rLuc mRNA-1 synthesis in the cells supporting replication of IGR-13 carrying GGGCAGCC, IGR-10 carrying GGGCUCGG, and IGR-11 carrying CCCGAGCC in place of the 8-nt sequence at nt 844 to 851, and we found that all mutants failed to accumulate rLuc mRNA-1 (Fig. 7B, IGR-1, IGR-13, IGR-10, and IGR-11), demonstrating that rLuc mRNA-1 accumulation required the CCCGUCGG sequence

at nt 844 to 851. Furthermore, accumulation of rLuc mRNA-1, but not rLuc mRNA-2, occurred in the cells supporting replication of IGR-16, which lacked the partial N gene ORF, the 8-nt sequence at nt 779 to 786, and 7 nt immediately downstream of the 8-nt sequence at nt 844 to 851, revealing that the 8-nt sequence at nt 779 to 786, which was complementary to another 8-nt sequence of CCCGUCGG at nt 844 to 851, was dispensable for rLuc mRNA-1 termination (Fig. 7B, IGR-16). These data also indicated the importance of the partial N gene ORF and the 8-nt sequence at nt 779 to 786 for rLuc mRNA-2 accumulation.

We next explored a possible mechanism that exerted rLuc mRNA-2 accumulation. Because the data shown above strongly suggested that transcriptional terminations of rLuc mRNA-1 and the N mRNA most probably used the same mechanism, we suspected that rLuc mRNA-2 accumulation was caused by the sequences that were found in the minigenomes and were absent in the viral S segment. To understand the importance of the sequence at nt 779 to 786 on rLuc mRNA-2 synthesis, we made IGR-12, which carried two 8-nt sequences, each of which was complementary to the 8-nt sequence at nt 844 to 851 and nt 779 to 786 (Fig. 7B, IGR-12). Neither rLuc mRNA-1 nor Luc mRNA-2 synthesis occurred in the cells supporting IGR-12 replication, suggesting that accumulation of rLuc mRNA-2 required the CCGACGGG sequence at nt 779 to 786; these data were consistent with those obtained from the analysis of IGR-16. We noted the presence of a CGUCGG sequence at nt 768 to 773 (dotted underlines in Fig. 7A), which was complementary to the 6 nt of the CCGACGGG sequence (the 6 nt are underlined) at nt 779 to 786. IGR-14, containing the GCAGCC sequence, which was complementary to the CGUCGG sequence at nt 768 to 773, and IGR-15, lacking the region at nt 758 to 776, which included the CGUCGG sequence, accumulated rLuc mRNA-1 in replicating cells, yet both failed to accumulate rLuc mRNA-2 (Fig. 7B, IGR-14 and IGR-15). These data suggested the importance of the presence of the CCGACGGG sequence at nt 779 to 786 and of its complementary CGUCGG sequence at nt 768 to 773 for rLuc mRNA-2 transcription termination.

The pentanucleotide sequence CGUCG was detected in the templates of the RNA corresponding to the termini of N, NSs, and M mRNAs of several phleboviruses, including RVFV (see Fig. 5); this pentanucleotide sequence was a part of the CCCGUCGG sequence at nt 844 to 851 of IGR-1. To test whether the CGUCG sequence within the CCCGUCGG sequence exerted rLuc mRNA-1 transcription termination, we constructed a new series of minigenomes (IGR-17, IGR-18, IGR-19, IGR-20, IGR-21, and IGR-22), all of which were derived from IGR-16; rLuc mRNA-1 accumulated in IGR-16-replicating cells, whereas rLuc mRNA-2 accumulation did not occur due to the deletion of the sequence from nt 758 to 786 (Fig. 7C). An efficient accumulation of rLuc mRNA-1 also occurred in the cells that support replication of IGR-20, whose sequence was similar to that of IGR-16, except that it carried the CGUCG sequence instead of the CCCGUCGG sequence, demonstrating that the pentanucleotide sequence CGUCG exerted rLuc mRNA-1 termination. We subsequently explored the significance of homopolymeric C-tract sequences that are present upstream of the transcription termination signal, the CGUCG sequence, for mRNA termination. Removal of sequences, including homopolymeric C tracts between nt 787 and 835, did not severely inhibit rLuc mRNA-1 accumulation (Fig. 7C, IGR-17 and IGR-18), yet deletion of an additional 8 nt, which included seven C nucleotides, immediately upstream of the CCCGUCGG sequence at nt 844 to 851 abolished the Luc mRNA-1 transcriptional termination (Fig. 7C, IGR-19), demonstrating the importance of the poly(C) sequence immediately upstream of the CCCGUCGG sequence. However, the presence of this poly(C) sequence was not sufficient to accumulate rLuc mRNA-1, as rLuc mRNA-1 did not occur in the cells supporting replication of IGR-22, which lacked the CCCGUCGG sequence at nt 844 to 851 (Fig. 7C, IGR-22). These data revealed that the presence of both the CGUCG sequence and its upstream poly(C)-rich 8-nt region was essential for rLuc mRNA-1 transcriptional termination.

Analysis of NSs mRNA transcription termination control. To study RNA elements that control NSs mRNA termination, we constructed a pPro-T7-mSv-based plasmid, NS IGR-1. The S-IGR was inserted at an orientation in NS IGR-1 opposite that of the IGR-1-based minigenomes described above, while the S-IGR used for the NS IGR-1 construction contained the S-IGR from nt 777 to 858 and lacked the short sequence of the N ORF (Fig. 8). The dotted line with terminal arrows in NS IGR-1 represents the NSs mRNA termination site (Fig. 8). NS IGR-1 replication resulted in rLuc mRNA accumulation. Analysis of NS IGR-2 and NS IGR-3, each of which carried a different-sized deletion upstream of an 8-nt-long CCCGUCGG sequence, showed that removal of the region from nt 858 to the immediate upstream nucleotide of the NSs mRNA termination site had only a small effect on Luc mRNA termination efficiency, whereas removal of the G-rich 8 nt within the NSs mRNA termination region reduced rLuc mRNA accumulation, indicating the importance of the poly(G)-rich 8-nt region for efficient mRNA transcription termination (Fig. 8, NS IGR-4). The replacement of the 8-nt sequence 3′-CCCGUCGGG-5′ with 3′-CGUCG-5′ slightly reduced rLuc mRNA accumulation efficiency (Fig. 8, compare NS IGR-2 to NS IGR-5), while the deletion of the 8-nt sequence abolished the transcriptional termination (Fig. 8, NS IGR-6). These data suggested the importance of the homoporimeric G tract and the 8-nt sequence, including 3′-CGUCG-5′, for NSs mRNA transcription termination. Overall, analysis of IGR-1- and NS IGR-1-derived minigenomes highlighted the importance of the transcription termination signal CGUCG and its upstream poly(C)- or poly(G)-rich sequence for transcription terminations of N and NSs mRNAs.

Analysis of M mRNA transcription termination control. An RNA element(s) that controls M mRNA transcriptional termination was examined by using pPro-T7-mSv-derived MUTR-1, which carried most of the M-5′ UTR, except for the very 5′-terminal 8 nt, and its mutants (Fig. 9). In Fig. 9, a dotted line with terminal arrows in MUTR-1 illustrates the M mRNA termination site (see also Fig. 3B), which is rich in C nucleotides. Two boxed regions represent two partially overlapping sequences, a 6-nt sequence, CCGUCG, and the pentanucleotide CGUCG sequence, both of which form the sequence CCGUCGUCG at nt 3778 to 3786. As pointed out above, the 6-nt sequence, CCGUCG, was included in the 8-nt sequence, CCCGUCGG, which was detected in the N-5′ UTR and in the NSs-5′ UTR. Northern blot analysis of MUTR-1

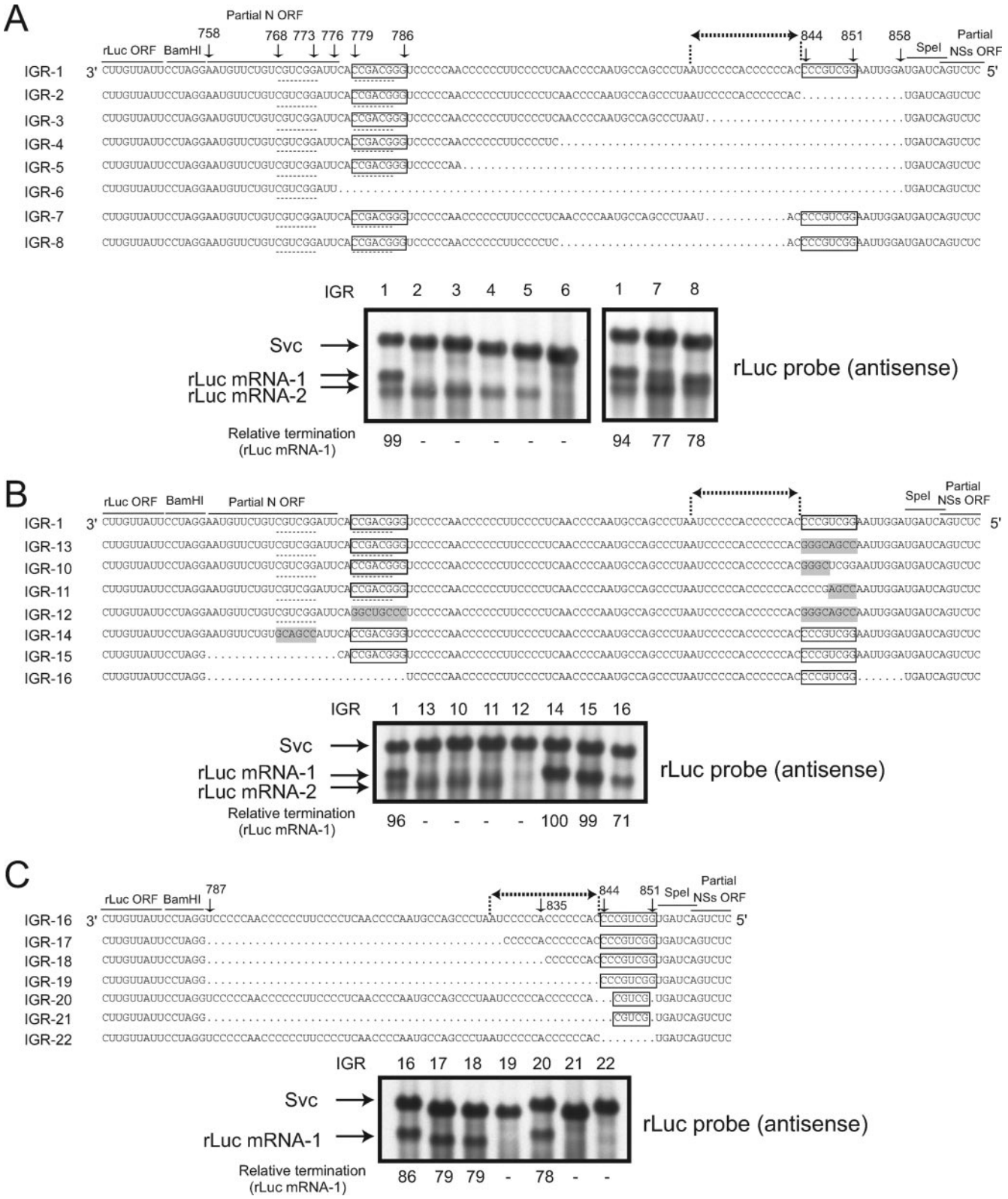

FIG. 7. Analysis of N mRNA transcription termination control. The S-IGR sequences in IGR-1 to IGR-8 (A), IGR-1 and IGR-13 to IGR-16 (B), and IGR16 to IGR-22 (C) are shown. The conserved 3′-CCCGUCGG-5′ and 3′-CCGACGGG-5′ sequences are boxed. Dotted lines highlight a 6-nt sequence (5′-CGUCGG-3′) that is complementary with the 3′-CCGACGGG-5′ sequence (see Discussion). The N mRNA termination site is denoted by dotted lines with terminal arrows. Shading indicates mutations that were introduced into IGR-10, IGR-11, IGR-12, IGR-13, and IGR-14. Intracellular RNAs were extracted from subconfluent BHK/T7-9 cells that were transfected with pT7-vN, pT7-vL, pCAGGS-vG, and plasmids carrying each minigenome at 48 h posttransfection. Northern blot analysis was performed using an rLuc probe that bound to the sense

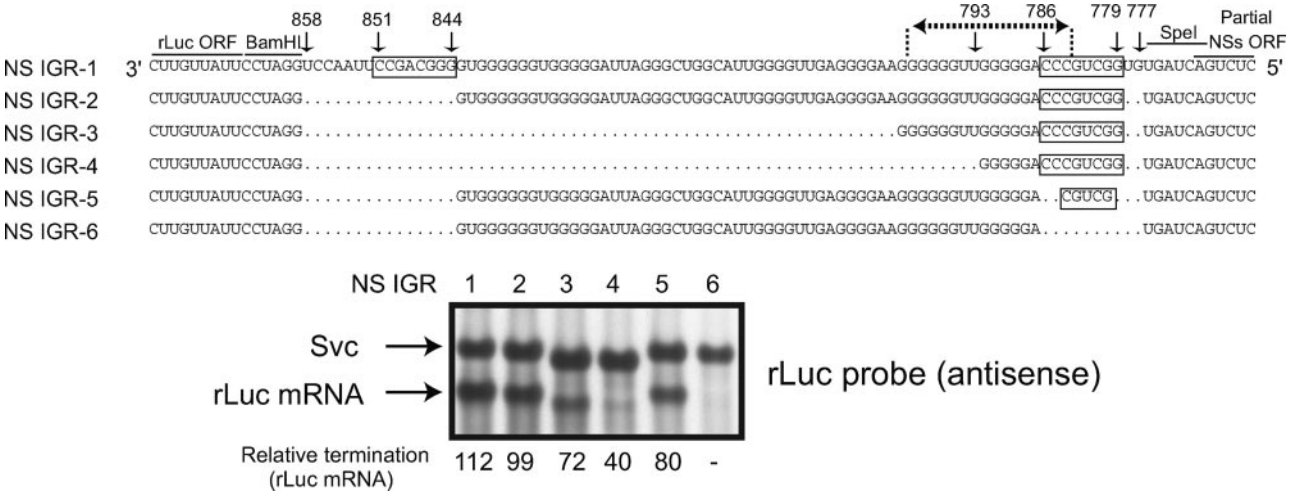

FIG. 8. Analysis of NSs mRNA transcription termination control. The S-IGR sequences in NS IGR-1 and other mutants are shown. The conserved 3′-CCCGUCGG-5′ and 3′-CCGACGGG-5′ sequences are boxed. The NSs mRNA termination site is denoted by a dotted line with terminal arrows. Svc represents the anti-virus-sense minigenome. The numbers represent the nucleotide positions of the S-IGR from the 3′ end of the virus-sense S segment. The rLuc probe was used for Northern blot analysis (see the legend to Fig. 7). The efficiency of the rLuc mRNA transcriptional termination of each minigenome (relative termination) was determined as described in the legend to Fig. 7.

and its mutants, each of which had a truncated M-5′ UTR starting at nt 3803 and extending to various lengths in the 3′ direction, showed that all mutants replicated. Many of them produced rLuc mRNA, including MUTR-6 carrying the 6-nt sequence, whereas rLuc mRNA termination did not occur in MUTR-7 and MUTR-8; MUTR-7 contained only one nucleotide in the 6-nt sequence, and MUTR-8 lacked both the 6-nt sequence and the pentanucleotides (Fig. 9A). These data suggested that transcriptional termination of the M-5′ UTR required the 6-nt sequence CCGUCG, which included the pentanucleotide CGUCG sequence.

Because the presence of polymeric C and G tracts was important for the efficient transcriptional termination in the N-5′ UTR and the NSs-5′ UTR, respectively (Fig. 7 and 8), we next tested whether the homopolymeric C tracts that existed immediately upstream of the pentanucleotides of the M-5′ UTR contributed to the transcription termination. Four different mutants, MUTR-9, MUTR-10, MUTR-11, and MUTR-12, each of which had a deletion of a different length within the homopolymeric C tracts of MUTR-6, were constructed and examined for rLuc mRNA transcription termination (Fig. 9B, MUTR-9 to MUTR-12). rLuc mRNA accumulation occurred in all of the mutants, including MUTR-12. In repeated experiments, amounts of the rLuc mRNA of MUTR-11 and that of MUTR-12 were smaller than those of rLuc mRNAs from MUTR-6, MUTR-9, or MUTR-10. MUTR-11 and MUTR-12 lacked sequences in homopolymeric C tracts that were present in the other mutants; these data suggested that the homopolymeric C tract promoted the transcription termination.

Characterization of MUTR-13, MUTR-14, and MUTR-15 containing homopolymeric G sequences, homopolymeric A sequences, and homopolymeric U sequences, respectively, in place of the homopolymeric C tracts suggested that homopolymeric G sequences exerted efficient mRNA transcription termination, while replacement of homopolymeric U sequences resulted in a low level of mRNA accumulation (Fig. 9B, MUTR-13 and MUTR-15). In the cells expressing MUTR-14 RNA, we repeatedly failed to detect an accumulation of rLuc mRNA and observed accumulation of a diffuse signal that migrated slightly more slowly than did that of the replicating minigenome (Fig. 9B, MUTR-14). The structure of the diffuse RNA signal is presently unclear. MUTR-14 carrying a continuous homopolymeric A tract (16 A nucleotides) at the M-5′ UTR failed to accumulate rLuc mRNA, whereas rLuc mRNA accumulation occurred in the cells supporting replication of MUTR-13 and MUTR-15, both of which had interrupted homopolymeric sequences. To know whether the presence of a continuous homopolymeric sequence suppressed rLuc mRNA termination, MUTR-14″, carrying an interrupted homopolymeric A sequence, and MUTR-15″, carrying a continuous homopolymeric U sequence (18 U nucleotides), were generated (Fig. 9B). A low level of rLuc mRNA accumulation occurred in the cells supporting replication of MUTR-14″ but did not occur in those supporting MUTR-15″ replication. Like MUTR-14, the MUTR-15″ minigenome appeared as a slowly migrating, diffuse signal in the gel. It seems that the presence of a continuous, long homopolymeric A or U sequence interfered with rLuc mRNA termination and affected the structure of the replicating minigenome. These results suggested the importance of the interrupted homopolymeric sequence that local-

rLuc gene ORF to detect the anti-virus-sense minigenome (Svc) as well as rLuc mRNA-1 and rLuc mRNA-2. The nucleotide positions of the S-IGR and the partial N ORF from the 3′ end of the virus-sense S segment are shown. The intensities of the rLuc mRNA-1 signal and the Svc signal of each minigenome were quantitated by densitometric scanning, and the abundance of rLuc mRNA-1 was normalized to that of Svc. These are shown as percentages of the Svc signal (relative termination) below each lane.

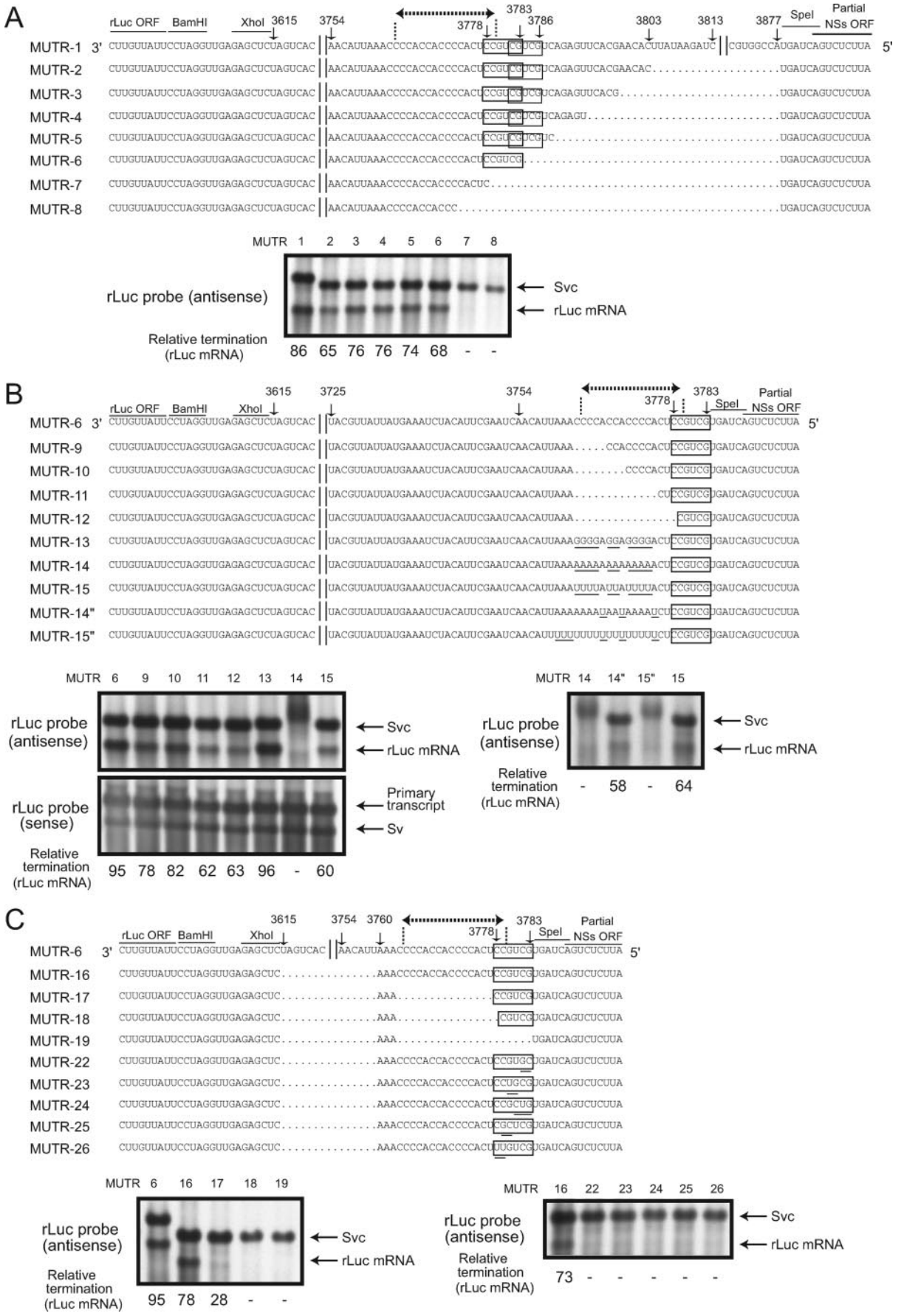
A
rLuc ORF
BamHI
XhoI
3615
3754
3778
3783
3786
3803
3813
3877
SpeI
Partial NSs ORF
MUTR-1
MUTR-2
MUTR-3
MUTR-4
MUTR-5
MUTR-6
MUTR-7
MUTR-8
MUTR 1 2 3 4 5 6 7 8
rLuc probe (antisense)
Svc
rLuc mRNA
Relative termination (rLuc mRNA)
86 65 76 76 74 68 - -
B
3615
3725
3754
3778
3783
SpeI
Partial NSs ORF
MUTR-6
MUTR-9
MUTR-10
MUTR-11
MUTR-12
MUTR-13
MUTR-14
MUTR-15
MUTR-14"
MUTR-15"
MUTR 6 9 10 11 12 13 14 15
rLuc probe (antisense)
Svc
rLuc mRNA
rLuc probe (sense)
Primary transcript
Sv
Relative termination (rLuc mRNA)
95 78 82 62 63 96 - 60
MUTR 14 14" 15" 15
rLuc probe (antisense)
Svc
rLuc mRNA
Relative termination (rLuc mRNA)
- 58 - 64
C
3615
3754
3760
3778
3783
SpeI
Partial NSs ORF
MUTR-6
MUTR-16
MUTR-17
MUTR-18
MUTR-19
MUTR-22
MUTR-23
MUTR-24
MUTR-25
MUTR-26
MUTR 6 16 17 18 19
rLuc probe (antisense)
Svc
rLuc mRNA
Relative termination (rLuc mRNA)
95 78 28 - -
MUTR 16 22 23 24 25 26
rLuc probe (antisense)
Svc
rLuc mRNA
Relative termination (rLuc mRNA)
73 - - - - -

ized immediately upstream of the CGUCG pentanucleotides for M mRNA transcription termination.

We further examined the role of the sequence that was located upstream of the M mRNA terminus for transcription termination (Fig. 9C, IGR-16 to IGR-19). Analysis of MUTR-16, which had a long deletion from nt 3615 to 3759, showed efficient rLuc mRNA accumulation. In contrast, efficient rLuc mRNA transcriptional termination was inhibited in the cells supporting replication of MUTR-17, which had an additional deletion immediately upstream of the 6-nt sequence CCGUCG. Alteration of the 6-nt sequence of MUTR-17 to the CGUCG pentanucleotide (MUTR-18) or removal of the CGUCG pentanucleotide abolished rLuc mRNA transcriptional termination (MUTR-19). Because MUTR-12 (Fig. 9B), which had the same deletion as MUTR-18 except that it contained the region from nt 3615 to 3759, had a higher level of rLuc mRNA accumulation, the absence of rLuc mRNA in MUTR-18 indicated that the region from nt 3615 to 3759 had a role in transcriptional termination. However, this effect was only evident when the sequence immediately upstream of the CGUCG pentanucleotides was removed. These data further emphasized the importance of the CGUCG pentanucleotides and its upstream homopolymeric C tracts for M mRNA transcription termination. To establish the importance of the 6-nt sequence, we constructed CCGUCG for transcription termination; MUTR-22, MUTR-23, MUTR-24, and MUTR-25, all of which had a scrambled version of the 6-nt sequence; and MUTR-26, carrying two nucleotide substitutions in the 6-nt sequence (Fig. 9C). All failed to accumulate rLuc mRNA, thereby demonstrating the importance of the CCGUCG sequence for transcriptional termination in the M-5′ UTR.

Analysis of L mRNA transcription termination control. The L-5′ UTR contained neither homopolymeric C tracts nor the CGUCG pentanucleotides (Fig. 10A). Instead, it had two 13-nt-long, complete complementary regions (the boxed sequences in Fig. 10A), and one of them at nt 6366 to 6378 (the downstream 13-nt-long region) existed within the region corresponding to the 3′ end of the L mRNA (Fig. 10A, a dotted line with terminal arrows). To study the mechanisms of L mRNA transcription termination, LUTR-1 was generated by inserting the entire L-5′ UTR, except for the terminal 8 nt, into pPro-T7-mSv. Northern blot analysis showed efficient LUTR-1 replication and rLuc mRNA accumulation (Fig. 10A). Subsequently, LUTR-6 and LUTR-7, each of which had a different-length deletion from the 5′ terminus of the inserted L-5′ UTR, were constructed (Fig. 10A). Replication of both minigenomes resulted in rLuc mRNA accumulation, demonstrating that the presence of the two entire 13-nt-long, complete complementary regions was not a requirement for rLuc mRNA termination.

We subsequently made LUTR-8 and LUTR-9. The 13-nt-long region at nt 6333 to 6345 (the upstream 13-nt region) of LUTR-8 and the downstream 13-nt-long region of LUTR-9 were replaced with the complementary sequences of the corresponding 13-nt-long region of LUTR-1; the two 13-nt-long regions in LUTR-8 and LUTR-9 were not complementary to each other. Both mutants underwent RNA replication, yet both failed to achieve rLuc mRNA accumulation (Fig. 10A). LUTR-10, in which each of the two 13-nt-long regions of LUTR-1 was converted into its complementary sequence, underwent RNA replication and rLuc mRNA accumulation. Similarly, LUTR-11, in which the upstream 13-nt region was replaced with the downstream 13-nt region, and LUTR-12, in which the downstream 13-nt region was replaced with the upstream 13-nt region, failed to accumulate rLuc mRNA, whereas rLuc mRNA accumulation occurred in the cells that supported replication of LUTR-13, in which the upstream 13-nt region was replaced with the downstream 13-nt region and the downstream 13-nt region was replaced with the upstream 13-nt region. These data suggested the importance of sequence complementarities of the two 13-nt-long regions, rather than their sequences, for rLuc mRNA termination.

Analysis of LUTR-6 and LUTR-7 demonstrated that the presence of the two entire 13-nt-long complete complementary regions was not needed for rLuc mRNA termination, while the analysis of other mutants suggested the importance of the sequence complementarities of the two 13-nt-long regions for rLuc mRNA termination. We tested whether an RNA secondary structure(s), which may present the nascent L mRNA, could exert transcriptional termination by examining the computer-predicted RNA secondary structures of the region from nt 6324 to 6389 of the nascent rLuc mRNA of LUTR-1 and those of its mutants. We were particularly interested in examining an RNA secondary structure that was generated by the two complementary regions in LUTR-1 and structures that were produced by the corresponding regions of the mutants (Fig. 10B). The two 13-nt regions that were present in the nascent rLuc mRNAs of LUTR-1, LUTR-10, and LUTR-13, all of which were capable of terminating mRNA transcription, formed a stable stem structure. LUTR-6 and LUTR-7 also accumulated rLuc mRNAs in replicating cells (Fig. 10A), and the formation of two different stem structures was predicted in the two 13-nt regions of their nascent rLuc mRNAs (Fig. 10B). We noted that the nascent mRNAs of LUTR-1 and its mutants

FIG. 9. Analysis of M mRNA transcription termination control. The M-5′ UTR sequences in MUTR-1 to MUTR-8 (A); MUTR-6, MUTR-9 to MUTR-15, MUTR-14″, and MUTR-15″ (B); and MUTR-6, MUTR-16 to MUTR-19, and MUTR-22 to MUTR-26 (C) are shown. The numbers represent the nucleotide positions of the M-5′ UTR from the 3′ end of the virus-sense M segment. The conserved 3′-CCGUCG-5′ sequence and an overlapping 3′-CGUCG-5′ sequence are indicated by boxes. The M mRNA transcriptional termination site is indicated by dotted lines with terminal arrows. The underlining of nucleotides in MUTR-13, MUTR-14, and MUTR-15 represents the replacement of the polymeric C sequence with polymeric G, A, and U sequences, respectively. Sequence differences between MUTR-14″ and MUTR-14 and those between MUTR-15 and MUTR-15″ are indicated by the underlined U nucleotides in MUTR-14″ and MUTR-15″, respectively. Northern blot analysis using intracellular RNAs of minigenome-replicating cells was performed using a probe that bound to the sense rLuc gene ORF (antisense) and another probe that bound to the antisense rLuc gene ORF (sense). The primary transcript, virus-sense S-like minigenomes (Sv), anti-virus-sense S-like minigenomes (Svc), and rLuc mRNA are shown. The efficiency of rLuc mRNA transcriptional termination of each minigenome (relative termination) was determined as described in the legend to Fig. 7.

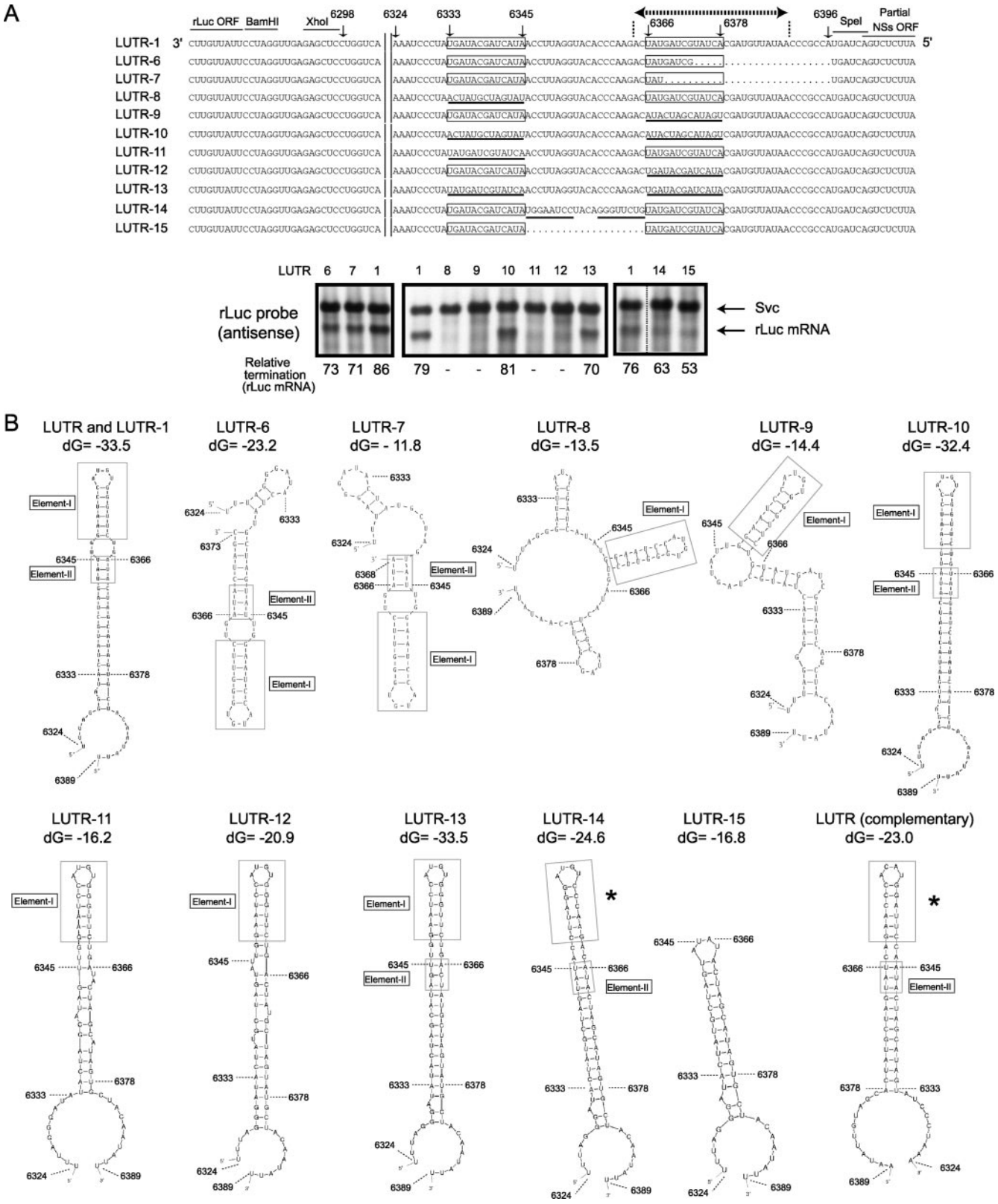

FIG. 10. Analysis of L mRNA transcription termination control. (A) L-5′ UTR sequences in LUTR-1 and other mutants are shown. The numbers represent the nucleotide positions of the L-5′ UTR from the 3′ end of the virus-sense L segment. The 13-nt-long regions are contained in boxes, and the L mRNA transcriptional termination site is denoted by dotted lines with terminal arrows. The underlined nucleotides represent the mutated nucleotides that were introduced into LUTR-8, LUTR-9, LUTR-10, LUTR-11, LUTR-12, LUTR-13, LUTR-14, and LUTR-15. Northern blot analyses using intracellular RNAs from minigenome-replicating cells were performed using a probe that bound to the sense rLuc

(LUTR-6 to LUTR-13) all formed a stem-loop structure (element I) (Fig. 10B, element I box) that was made by nt 6348 to 6363. Furthermore, the nascent rLuc mRNAs that underwent transcriptional termination shared a short stem structure consisting of nt 6366 to 6368 and nt 6343 to 6345 (element II) (Fig. 10B, boxed regions). In contrast, element II was missing from the nascent rLuc mRNAs of LUTR-8, LUTR-9, LUTR-11, and LUTR-12, all of which failed to terminate transcription. To know the role of the sequence between the two 13-nt-long, complete complementary regions for transcription termination, LUTR-14 and LUTR-15 were generated; LUTR-14 had two 8-nt-long regions that were complementary to the corresponding parts of LUTR-1, while LUTR-15 lacked the entire region between the two 13-nt-long complete complementary sequences (Fig. 10B). The nascent rLuc mRNA of LUTR-14 formed element II and an RNA element, which was structurally similar to element I. The nascent rLuc mRNA of LUTR-15 lacked both elements I and II yet still had a stable stem-loop structure that included RNA elements similar to those of elements I and II. Replication of LUTR-14 and LUTR-15 resulted in low levels of rLuc mRNA accumulation (Fig. 9A). These data suggested the importance of the presence of both element I and element II or similar RNA elements in the nascent mRNA for L mRNA transcriptional termination.

DISCUSSION

Identification of the 3′ ends of RVFV mRNAs. To understand RVFV transcription termination, we first identified the transcriptional termination sites of all RVFV mRNA species. Using RPAs, we mapped the 3′ end of the N mRNA at nt 828 to 843 from the 3′ end of the virus-sense S segment, that of the NSs mRNA at nt 784 to 799 from the 3′ end of the virus-sense S segment, and that of the M mRNA at nt 3764 to 3779 from the 3′ end of the virus-sense M segment. The 3′ termini of N, NSs, and M mRNAs that were determined here were consistent with those reported previously by others (1, 11). Like UUKV (44), TOSV (21), and *Tospovirus* (46), the 3′ termini of RVFV N and NSs mRNAs were found to have regions (a range of 30 to 60 nt in length; Fig. 3A) that were complementary to one another; these complementary regions, ranging in length from 30 to 60 nt, potentially form a double-stranded structure between N mRNA and NSs mRNA in infected cells. Because double-stranded RNAs are known to trigger host innate immune responses and translation inhibition (22), further studies are warranted to explore the biological significance of the sequence complementarity at the 3′ termini of RVFV N and NSs mRNAs.

It has been reported that the 3′ terminus of the L mRNA of Sin Nombre virus, a hantavirus, is the full-length complement of the 5′ end of the viral L RNA segment (24). Albarino et al. examined the 3′ terminus of the RVFV L mRNA by using the 3′RACE method and concluded that L mRNA termination occurred at the end of the L-5′ UTR (1). In contrast, our present RPA of intracellular RNAs from MP-12- and rMP12-LUTR-infected cells determined the 3′ end of L mRNA to be at nt 6364 to 6389 of the virus-sense L-segment RNA. Analysis of various minigenomes carrying the L-5′ UTR region further identified RNA elements that were important for L mRNA termination. Our finding that the 3′ end of RVFV L mRNA was truncated compared to that of the virus-sense L-segment RNA suggests that transcriptional termination of L mRNA differs among bunyaviruses.

Mechanisms of RVFV mRNA transcription termination. Experiments using pPro-T7-mSv-derived plasmids containing the S-IGR or the M-5′ UTR suggested that the CGUCG pentanucleotides play a critical role in the transcription termination of N, NSs, and M mRNAs; no mRNA accumulation occurred in minigenomes lacking the CGUCG pentanucleotides (IGR-12, IGR-22, NS IGR-6, MUTR-7, and MUTR-8) and those carrying mutated CGUCG pentanucleotides (MUTR-22, MUTR-23, MUTR-24, MUTR-25, and MUTR-26) in the M-5′ UTR. We also found the presence of the same pentanucleotides downstream within 10 nucleotides of the transcriptional termination sites of the N mRNAs of LaCrosse virus, snowshoe hare virus, and Germiston virus, belonging to genus *Orthobunyavirus*, and the M mRNA of Germiston virus (data not shown), implying that the CGUCG pentanucleotides also may exert transcription terminations of these mRNAs. A study using a minigenome of Bunyamwera virus showed the importance of a 6-nt GUCGAC sequence at the N-5′ UTR for transcription termination (4). Furthermore, Maguari, Northway, Batai, Cache Valley, and Bunyamwera viruses, belonging to the Bunyamwera serogroup, and Lumbo virus, belonging to the California serogroup, in the genus *Orthobunyavirus* carry a UGUCG sequence (shared sequence is underlined), which shares the sequence within the 6-nt GUCGAC sequence, at their S-5′ UTRs (4), implying the importance of UGUCG or related sequences for transcription termination in these viruses. In contrast, the NSs-5′ UTR of PTV and the N-5′ UTR of the tick-borne UUKV have neither CGUCG nor UGUCG pentanucleotide sequences near the transcriptional termination sites (20). Giorgi et al. suggested that the S-IGRs of these

gene ORF (antisense). The anti-virus-sense S-like minigenome (Svc) and rLuc mRNA are shown. The efficiency of rLuc mRNA transcriptional termination of each minigenome (relative termination) was determined as described in the legend to Fig. 7. (B) The computer-predicted RNA secondary structures of the region from nt 6324 to 6389 of the nascent rLuc mRNAs of LUTR-1, LUTR-8, LUTR-9, LUTR-10, LUTR-11, LUTR-12, LUTR-13, LUTR-14, and LUTR-15, from nt 6324 to 6373 of that of LUTR-6, and from nt 6324 to 6368 of that of LUTR-7. The RNA secondary structure of the corresponding region of the nascent rLuc mRNA of rMP12-LUTR (see the legend to Fig. 4) is shown as LUTR (complementary). The most energetically stable structures at 37°C are shown. The RNA secondary analysis of LUTR-1 and its mutants used the anti-virus-sense RNA sequence, while that of LUTR (complementary) used the virus-sense RNA sequence. Nucleotide positions corresponding to LUTR-1 are shown in the structures. Boxes represent the L mRNA termination element, which consisted of nt 6366 to 6368 and nt 634 to 6345. Elements I and II are shown in boxes. The asterisks represent an RNA secondary structure that is similar to element I. dG, initial free energy (kcal/mol).

viruses, but not of RVFV, TOSV, and sandfly fever Sicilian virus, may form stable RNA secondary structures (20). These predicted stable RNA secondary structures may be important for mRNA transcriptional termination in the S segments of PTV and UUKV. However, further studies are required to test this possibility. Results in the present study and those in past reports suggest that transcriptional terminations of the N, NSs, and M mRNAs of many viruses, if not all, belonging to the orthobunyaviruses and phleboviruses require the presence of a specific 5-nt- or 6-nt-long sequence, the specificity of which may vary among different viruses.

Our studies further suggested that polymeric C or G sequences, which exist upstream of the CGUCG pentanucleotides, were important for efficient transcriptional termination (IGR-19, IGR-21, NS IGR-4, MUTR-17, and MUTR-18). The experiments that tested the effects of the replacement of the polymeric C tract with the polymeric G, U, or A tract in the M-5′ UTR (MUTR-6, MUTR-13, MUTR-14, and MUTR-15) revealed that the polymeric C or G tract worked better than the polymeric U or A tract for transcriptional termination. Other bunyaviruses also carry homopolymeric sequences near transcription termination sites. The N-5′ UTRs of TOSV and sandfly fever Sicilian virus contain long homopolymeric C sequences, and the NSs-5′ UTRs of both viruses carry long homopolymeric G sequences. The M-5′ UTR of snowshoe hare virus also contains a homopolymeric C tract near the termination site, while the termination site of Germiston virus contains a homopolymeric U tract (data not shown). Taken together, these data imply the importance of the homopolymeric sequence in transcriptional termination in bunyaviruses. How do homopolymeric C/G sequences promote RVFV mRNA termination? DNA-dependent RNA polymerases of prokaryotes and eukaryotes undergo slippage during transcription of homopolymeric sequences (45). Likewise, RNA-dependent RNA polymerases of negative-strand RNA viruses undergo a similar slippage during transcription (6, 29). For example, vesicular stomatitis virus polymerase terminates its transcription with 3′-AUACU$_7$-5′, and the slippage of polymerase at the U$_7$ is a prerequisite for the termination and polyadenylation of viral mRNAs. It is possible that the RVFV L protein also undergoes slippage at the homopolymeric tracts of the G or C sequence upstream of a 5-nt- or 6-nt-long sequence of the transcription termination signal, e.g., the CGUCG pentanucleotides. A putative slippage of L protein at homopolymeric tracts of the G or C sequence may induce a transcriptional attenuation, leading to an efficient transcription termination at the transcription termination signal.

Although homopolymeric sequences in front of the CGUCG pentanucleotides promoted RVFV mRNA termination, both MUTR-14, carrying 16 continuous A nucleotides, and MUTR-15″, carrying 18 continuous U nucleotides, failed to accumulate mRNAs (Fig. 9B). Minigenomes of MUTR-14 and MUTR-15″ also appeared as slowly migrating diffuse signals in the gels. In contrast, interruptions of the long continuous homopolymeric A or U sequence restored mRNA termination (MUTR-15 and MUTR-14″) and resulted in the accumulation of minigenome RNA that appeared as a discrete signal in the gel (Fig. 9B). These data suggested that the presence of long, continuous homopolymeric A and U sequences interfered with rLuc mRNA termination and affected the structure of the replicating minigenome. It is possible that, for efficient viral RNA replication and mRNA termination in the S and M segments, homopolymeric C/G sequences that exist in front of the CGUCG pentanucleotides need to include other nucleotides to prevent forming very long continuous homopolymeric sequences.

Mutant minigenomes, including IGR-6, IGR-12, IGR-19, IGR-22, NS IGR-6, MUTR-7, MUTR-8, MUTR-18, MUTR-19, LUTR-8, LUTR-9, LUTR-11, and LUTR-12, failed to accumulate rLuc mRNA in replicating cells. We suspected that in the cells supporting replication of these minigenomes, mRNA synthesis occurred and transcription terminated at the end of the template RNA; transcription termination did not occur in the middle of the template RNA in these minigenomes. To further confirm this possibility, we examined the rLuc activities in the cells supporting replication of those minigenome RNAs. High levels of rLuc activities were detected in the cells supporting replication of all of these minigenomes, whereas cells transfected with only pPro-T7-mSv-IGR-1 produced only a background level of rLuc activities (data not shown). These data suggested that mRNAs were in fact transcribed from these replicating minigenomes, yet RNA transcription machinery failed to terminate mRNA transcription in the middle of the template and continued mRNA transcription until the 5′ end of the template. These data further suggest that viral mRNAs carrying extra sequences, which did not exist in authentic viral mRNAs, at their 3′ ends were translationally active.

Accumulation of two mRNAs, rLuc mRNA-1 and rLuc mRNA-2, occurred in the cells supporting the replication of IGR-1 (Fig. 7). Our experiments strongly suggested that transcriptional terminations of rLuc mRNA-1 and N mRNA most probably used the same mechanism. We explored a possible mechanism of Luc mRNA-2 transcription termination by using IGR-12, IGR-14, IGR-15, and IGR-16 and found that the presence of the CCGACGGG sequence at nt 779 to 786 and its complementary CGUCGG sequence at nt 768 to 773 was important for rLuc mRNA-2 transcription termination; it is possible that the CGUCGG sequence and the CCGACGGG sequence form an RNA stem structure in the nascent rLuc mRNAs of IGR-1. In IGR-1 and its mutants that generated rLuc mRNA-2, the rLuc gene ORF terminated upstream from the partial N gene ORF sequence shown in Fig. 7, and hence the partial N gene ORF sequence existed within an untranslated region in these minigenomes. In contrast, the N gene ORF ends only a few nucleotides upstream of the CCGACGGG sequence in the S-segment RNA of MP-12; the CGUCGG sequence exists within the N gene ORF (Fig. 3). It is hypothesized that associations of nascent bunyavirus mRNA with ribosomes prevent premature transcription termination; without this association, the nascent mRNA may interact with its template and stop mRNA elongation (7). Accordingly, a putative RNA stem structure, which was made by the CGUCGG sequence and the CCGACGGG sequence, near the end of the N gene ORF may be disrupted by the association of nascent N mRNA with ribosomes in RVFV-infected cells. In contrast, the same putative RNA stem structure in the nascent rLuc mRNA may not be disrupted, because this RNA structure was formed within the untranslated region and probably does not associate with ribosomes. We suspect that the

putative RNA stem structure, which probably existed in nascent rLuc mRNA of the minigenomes but not in the nascent N mRNA of the S segment, may contribute to the rLuc mRNA-2 accumulation in the cells supporting replication of IGR-1 and its mutants, which generated rLuc mRNA-2.

The L-5′ UTR contained neither homopolymeric C tracts nor the CGUCG pentanucleotides. Instead, it had two 13-nt-long regions that are complementary to each other. We found that rLuc mRNA termination still occurred after removal of 10 nt from the downstream 13-nt region at nucleotides 6366 to 6378, whereas analysis of other mutants demonstrated that the complementarities of the two 13-nt-long regions, rather than their sequences, were important for rLuc mRNA termination. These data imply that a secondary (or ternary) RNA structure that is comprised of the two 13-nt-long regions plays a critical role in L mRNA transcription termination. Computer-mediated modeling further suggested the importance of elements I and II for L mRNA transcriptional termination (Fig. 10B). Both RNA elements exist at the UTR. Accordingly, unlike N mRNA termination, as discussed above, it is expected that these RNA elements in the nascent L mRNA do not interact with ribosomes and should not be disrupted.

Our analysis of rMP12-LUTR, which contained most of the L-5′ UTR region and the rLuc ORF in place of the S-IGR and the NSs ORF, respectively, in the S segment showed N mRNA accumulation (Fig. 4). In addition, four minor RNA species, which probably represented mRNA species carrying the rLuc gene, were detected in rMP12-LUTR-infected cells (Fig. 4B, right panel). These data suggested that low levels of rLuc mRNA termination also occurred at four different sites within the inserted L-5′ UTR region of rMP12-LUTR. The computer-mediated prediction of the putative nascent rLuc mRNA of rMP12-LUTR at nt 6324 to 6389 demonstrated a long stem structure that included element II and an element I-like RNA stem-loop structure (Fig. 10B, LUTR complementary, indicated by an asterisk) that was composed of the complementary sequence of element I. Element I of LUTR-1 included a G-U wobble base pairing between nt 6351 and 6360, whereas no wobble base pairing was found in the element I-like structure of rLuc mRNA of rMP12-LUTR. This small difference in the RNA secondary structures between element I of LUTR-1 and the corresponding site of rLuc mRNA of rMP12-LUTR might have affected the strength of the transcriptional termination. Consistent with this notion, transcription termination of LUTR-14 was not efficient, and nascent mRNA of LUTR-14 could form an element I-like structure that lacked a G-U wobble base pairing (Fig. 10). Together, these data imply that viral RNA elements that govern L mRNA termination differ from those that regulate mRNA terminations in the M and S segments. Differential regulation of transcriptional termination for the three RNA segments is probably required for optimal RVFV replication in infected cells.

ACKNOWLEDGMENTS

This work was supported by grants from the NIAID to S.M. and C.J.P. through the Western Regional Center of Excellence for Biodefense and Emerging Infectious Diseases Research, NIH grant number U54 AI057156, and by a Collaborative Grant on Emerging Viral Diseases (NIH-NIAID-DMID-02-24). T.I. and S.W. were supported by the James W. McLaughlin Fellowship Fund.

REFERENCES

1. **Albarino, C. G., B. H. Bird, and S. T. Nichol.** 2007. A shared transcription termination signal on negative and ambisense RNA genome segments of Rift Valley fever, sandfly fever Sicilian, and Toscana viruses. J. Virol. **81:** 5246–5256.
2. **Balkhy, H. H., and Z. A. Memish.** 2003. Rift Valley fever: an uninvited zoonosis in the Arabian Peninsula. Int. J. Antimicrob. Agents **21:**153–157.
3. **Barr, J. N., J. W. Rodgers, and G. W. Wertz.** 2005. The Bunyamwera virus mRNA transcription signal resides within both the 3′ and the 5′ terminal regions and allows ambisense transcription from a model RNA segment. J. Virol. **79:**12602–12607.
4. **Barr, J. N., J. W. Rodgers, and G. W. Wertz.** 2006. Identification of the Bunyamwera bunyavirus transcription termination signal. J. Gen. Virol. **87:** 189–198.
5. **Barr, J. N., and G. W. Wertz.** 2005. Role of the conserved nucleotide mismatch within 3′- and 5′-terminal regions of Bunyamwera virus in signaling transcription. J. Virol. **79:**3586–3594.
6. **Barr, J. N., S. P. Whelan, and G. W. Wertz.** 1997. *cis*-Acting signals involved in termination of vesicular stomatitis virus mRNA synthesis include the conserved AUAC and the U7 signal for polyadenylation. J. Virol. **71:**8718–8725.
7. **Bellocq, C., R. Raju, J. Patterson, and D. Kolakofsky.** 1987. Translational requirement of La Crosse virus S-mRNA synthesis: in vitro studies. J. Virol. **61:**87–95.
8. **Bouloy, M., C. Janzen, P. Vialat, H. Khun, J. Pavlovic, M. Huerre, and O. Haller.** 2001. Genetic evidence for an interferon-antagonistic function of Rift Valley fever virus nonstructural protein NSs. J. Virol. **75:**1371–1377.
9. **Bouloy, M., N. Pardigon, P. Vialat, S. Gerbaud, and M. Girard.** 1990. Characterization of the 5′ and 3′ ends of viral messenger RNAs isolated from BHK21 cells infected with Germiston virus (Bunyavirus). Virology **175:**50–58.
10. **Bouloy, M., P. Vialat, M. Girard, and N. Pardigon.** 1984. A transcript from the S segment of the Germiston bunyavirus is uncapped and codes for the nucleoprotein and a nonstructural protein. J. Virol. **49:**717–723.
11. **Collett, M. S.** 1986. Messenger RNA of the M segment RNA of Rift Valley fever virus. Virology **151:**151–156.
12. **Emery, V. C., and D. H. L. Bishop.** 1987. Characterization of Punta Toro S mRNA species and identification of an inverted complementary sequence in the intergenic region of Punta Toro phlebovirus ambisense S RNA that is involved in mRNA transcription termination. Virology **156:**1–11.
13. **Eshita, Y., B. Ericson, V. Romanowski, and D. H. Bishop.** 1985. Analyses of the mRNA transcription processes of snowshoe hare bunyavirus S and M RNA species. J. Virol. **55:**681–689.
14. **Flick, K., A. Katz, A. Overby, H. Feldmann, R. F. Pettersson, and R. Flick.** 2004. Functional analysis of the noncoding regions of the Uukuniemi virus (*Bunyaviridae*) RNA segments. J. Virol. **78:**11726–11738.
15. **Flick, R., F. Elgh, and R. F. Pettersson.** 2002. Mutational analysis of the Uukuniemi virus (*Bunyaviridae* family) promoter reveals two elements of functional importance. J. Virol. **76:**10849–10860.
16. **Flick, R., and R. F. Pettersson.** 2001. Reverse genetics system for Uukuniemi virus (*Bunyaviridae*): RNA polymerase I-catalyzed expression of chimeric viral RNAs. J. Virol. **75:**1643–1655.
17. **Garcin, D., M. Lezzi, M. Dobbs, R. M. Elliott, C. Schmaljohn, C. Y. Kang, and D. Kolakofsky.** 1995. The 5′ ends of Hantaan virus (*Bunyaviridae*) RNAs suggest a prime-and-realign mechanism for the initiation of RNA synthesis. J. Virol. **69:**5754–5762.
18. **Gauliard, N., A. Billecocq, R. Flick, and M. Bouloy.** 2006. Rift Valley fever virus noncoding regions of L, M and S segments regulate RNA synthesis. Virology **351:**170–179.
19. **Gerrard, S. R., B. H. Bird, C. G. Albarino, and S. T. Nichol.** 2006. The NSm proteins of Rift Valley fever virus are dispensable for maturation, replication and infection. Virology **359:**459–465.
20. **Giorgi, C., L. Accardi, L. Nicoletti, M. C. Gro, K. Takehara, C. Hilditch, S. Morikawa, and D. H. Bishop.** 1991. Sequences and coding strategies of the S RNAs of Toscana and Rift Valley fever viruses compared to those of Punta Toro, Sicilian Sandfly fever, and Uukuniemi viruses. Virology **180:**738–753.
21. **Gro, M. C., P. Di Bonito, L. Accardi, and C. Giorgi.** 1992. Analysis of 3′ and 5′ ends of N and NSs messenger RNAs of Toscana phlebovirus. Virology **191:**435–438.
22. **Haller, O., G. Kochs, and F. Weber.** 2006. The interferon response circuit: induction and suppression by pathogenic viruses. Virology **344:**119–130.
23. **Hay, A. J., J. J. Skehel, and J. McCauley.** 1980. Structure and synthesis of influenza virus complementary RNAs. Philos. Trans. R. Soc. Lond. B **288:** 341–348.
24. **Hutchinson, K. L., C. J. Peters, and S. T. Nichol.** 1996. Sin Nombre virus mRNA synthesis. Virology **224:**139–149.
25. **Ikegami, T., C. J. Peters, and S. Makino.** 2005. Rift Valley fever virus nonstructural protein NSs promotes viral RNA replication and transcription in a minigenome system. J. Virol. **79:**5606–5615.
26. **Ikegami, T., S. Won, C. J. Peters, and S. Makino.** 2006. Rescue of infectious

Rift Valley fever virus entirely from cDNA, analysis of virus lacking the NSs gene, and expression of a foreign gene. J. Virol. **80:**2933–2940.
27. **Ikegami, T., S. Won, C. J. Peters, and S. Makino.** 2005. Rift Valley fever virus NSs mRNA is transcribed from an incoming anti-viral-sense S RNA segment. J. Virol. **79:**12106–12111.
28. **Ito, N., M. Takayama-Ito, K. Yamada, J. Hosokawa, M. Sugiyama, and N. Minamoto.** 2003. Improved recovery of rabies virus from cloned cDNA using a vaccinia virus-free reverse genetics system. Microbiol. Immunol. **47:**613–617.
29. **Jacques, J. P., S. Hausmann, and D. Kolakofsky.** 1994. Paramyxovirus mRNA editing leads to G deletions as well as insertions. EMBO J. **13:**5496–5503.
30. **Jin, H., and R. M. Elliott.** 1993. Characterization of Bunyamwera virus S RNA that is transcribed and replicated by the L protein expressed from recombinant vaccinia virus. J. Virol. **67:**1396–1404.
31. **Jin, H., and R. M. Elliott.** 1993. Non-viral sequences at the 5′ ends of Dugbe nairovirus S mRNAs. J. Gen. Virol. **74:**2293–2297.
32. **Kohl, A., E. F. Dunn, A. C. Lowen, and R. M. Elliott.** 2004. Complementarity, sequence and structural elements within the 3′ and 5′ non-coding regions of the Bunyamwera orthobunyavirus S segment determine promoter strength. J. Gen. Virol. **85:**3269–3278.
33. **Lai, M. M., P. R. Brayton, R. C. Armen, C. D. Patton, C. Pugh, and S. A. Stohlman.** 1981. Mouse hepatitis virus A59: mRNA structure and genetic localization of the sequence divergence from hepatotropic strain MHV-3. J. Virol. **39:**823–834.
34. **Le May, N., S. Dubaele, L. Proietti De Santis, A. Billecocq, M. Bouloy, and J. M. Egly.** 2004. TFIIH transcription factor, a target for the Rift Valley hemorrhagic fever virus. Cell **116:**541–550.
35. **Lopez, N., R. Muller, C. Prehaud, and M. Bouloy.** 1995. The L protein of Rift Valley fever virus can rescue viral ribonucleoproteins and transcribe synthetic genome-like RNA molecules. J. Virol. **69:**3972–3979.
36. **Meegan, J. M.** 1979. The Rift Valley fever epizootic in Egypt 1977–78. 1. Description of the epizootic and virological studies. Trans. R. Soc. Trop. Med. Hyg. **73:**618–623.
37. **Morvan, J., P. E. Rollin, S. Laventure, I. Rakotoarivony, and J. Roux.** 1992. Rift Valley fever epizootic in the central highlands of Madagascar. Res. Virol. **143:**407–415.
38. **Muller, R., J. F. Saluzzo, N. Lopez, T. Dreier, M. Turell, J. Smith, and M. Bouloy.** 1995. Characterization of clone 13, a naturally attenuated avirulent isolate of Rift Valley fever virus, which is altered in the small segment. Am. J. Trop. Med. Hyg. **53:**405–411.
39. **Pattnaik, A. K., and G. Abraham.** 1983. Identification of four complementary RNA species in Akabane virus-infected cells. J. Virol. **47:**452–462.
40. **Peters, C. J., and J. Meegan.** 1981. Rift Valley fever, p. 403–420. *In* G. W. Beran and H. H. Steele (ed.), Handbook series of zoonoses. Section B, viral zoonoses, vol. 1. CRC Press, Boca Raton, FL.
41. **Raju, R., L. Raju, D. Hacker, D. Garcin, R. Compans, and D. Kolakofsky.** 1990. Nontemplated bases at the 5′ ends of Tacaribe virus mRNAs. Virology **174:**53–59.
42. **Schmaljohn, C. S., and J. W. Hooper.** 2001. Bunyaviridae: the viruses and their replication, p. 1581–1602. *In* B. N. Fields and D. M. Knipe (ed.), Fields virology, 4th ed. Lippincott, Williams & Wilkins, Philadelphia, PA.
43. **Shoemaker, T., C. Boulianne, M. J. Vincent, L. Pezzanite, M. M. Al-Qahtani, Y. Al-Mazrou, A. S. Khan, P. E. Rollin, R. Swanepoel, T. G. Ksiazek, and S. T. Nichol.** 2002. Genetic analysis of viruses associated with emergence of Rift Valley fever in Saudi Arabia and Yemen, 2000–01. Emerg. Infect. Dis. **8:**1415–1420.
44. **Simons, J. F., and R. F. Pettersson.** 1991. Host-derived 5′ ends and overlapping complementary 3′ ends of the two mRNAs transcribed from the ambisense S segment of Uukuniemi virus. J. Virol. **65:**4741–4748.
45. **Uptain, S. M., C. M. Kane, and M. J. Chamberlin.** 1997. Basic mechanisms of transcript elongation and its regulation. Annu. Rev. Biochem. **66:**117–172.
46. **van Knippenberg, I., R. Goldbach, and R. Kormelink.** 2005. Tomato spotted wilt virus S-segment mRNAs have overlapping 3′ ends containing a predicted stem-loop structure and conserved sequence motif. Virus Res. **110:**125–131.
47. **Won, S., T. Ikegami, C. J. Peters, and S. Makino.** 2006. NSm and 78-kilodalton proteins of Rift Valley fever virus are nonessential for viral replication in cell culture. J. Virol. **80:**8274–8278.
48. **Zuker, M.** 2003. Mfold web server for nucleic acid folding and hybridization prediction. Nucleic Acids Res. **31:**3406–3415.